hydrology

MDPI

Review

Fluvial Characteristics of the Magdalena River (Colombia) and a Nature-Based Solution for Navigation Conditions

Allen Bateman Pinzón * and Raúl Sosa Pérez

Sediment Transport Research Group, Civil and Environmental Department, Barcelona Tech-University, Jordi Girona 31, 08034 Barcelona, Spain; raul.sosa@upc.edu

* Correspondence: allen.bateman@upc.edu; Tel.: +34-639217557

Abstract

This study analyzes the hydro-morphological dynamics of the lower 40 km of the Magdalena River (Colombia), with particular emphasis on the reach between Malambo and the river mouth at Bocas de Ceniza. Bathymetric profiles obtained from three field campaigns conducted between 2017 and 2018 were used to characterize riverbed morphology and to quantify the evolution of subaqueous bedforms (dunes) under different flow conditions. The results reveal a systematic increase in dune height and wavelength with increasing discharge. The dominant discharge during the observation period was approximately 7400 m^3/s, associated with a total measured sediment load of about 2000 kton/day, corresponding to a volumetric concentration of 0.12%. Variations in the Manning roughness coefficient were identified, ranging from 0.020 to 0.037, primarily driven by changes in discharge and, to a lesser extent, by spatial variability in hydraulic roughness, particularly in port areas. Bedforms exhibit significant growth during high-flow periods, consistent with findings reported in the literature. Analysis of mean velocity profiles indicates that the von Kármán coefficient varies with sediment concentration and turbulence intensity. Finally, a nature-based solution is proposed for the river mouth, consisting of reconfiguring the Thalweg in the final kilometers of the channel to replicate the meandering pattern of the adjacent bend. This intervention aims to enhance Thalweg stability, reduce saline wedge intrusion, promote sediment and flow dispersion toward the natural submarine canyon, and improve navigability at the river mouth.

Keywords: nature-based solution; von Kármán coefficient; sediment transport; navigation; dunes; saline wedge; thalweg

Academic Editors: Hao Chen, Linjing Qiu and Wenbin Ding

Received: 29 December 2025
Revised: 22 February 2026
Accepted: 25 February 2026
Published: 3 March 2026

1. Introduction

Transforming the Magdalena River for Navigation: River–Estuary Morphodynamics and Nature-Based Design Principles

Large alluvial rivers approaching the sea commonly exhibit strong interactions between upstream sediment supply, channel–bar morphodynamics, and estuarine and coastal boundary conditions. These coupled processes can impose persistent constraints on navigation, particularly where mouth bars, saline intrusion, and low-energy hydrodynamic conditions promote sediment trapping. In such systems, maintaining a deep and stable thalweg is not solely an engineering challenge but a morphodynamic one, shaped by river planform geometry, channel stability mechanisms, and river–estuary exchange processes [1]. The Magdalena River has been the focus of navigation-oriented interventions

since the late nineteenth century, reflecting its historical role as a strategic corridor between the Caribbean coast and the interior of Colombia.

Large sand-bed rivers have long been recognized as self-organizing morphodynamic systems in which channel geometry, sediment transport capacity, and discharge variability co-evolve toward quasi-equilibrium configurations [2,3]. In such systems, engineering attempts to impose fixed planforms or artificially enhanced depths may generate compensatory morphodynamic adjustments, including bar reorganization, slope modification, and altered sediment retention patterns [3].

Major engineering works intensified in the early twentieth century, most notably with the construction of the eastern and western breakwaters at the river mouth. These structures were designed to concentrate flow and suppress the natural tendency toward a distributary, island-rich deltaic configuration. While such training works can locally enhance conveyance, they may also alter the balance among discharge, sediment transport capacity, and along-channel slope, thereby affecting bar dynamics and the stability of the navigable corridor [4,5]. A key metric for navigation reliability is thalweg persistence. In many alluvial rivers, sinuous planforms promote a more persistent deep thread through curvature-driven secondary circulation [6,7], whereas long straight reaches often exhibit frequent lateral thalweg shifts and bar-induced shoaling [3,8].

Additional complexity arises from the river–estuary interaction at the mouth of the Magdalena River in the Caribbean Sea. A saline wedge develops that can penetrate up to approximately 21 km upstream during low-flow conditions (around 3000 m^3/s) and retreat to 2–3 km during high flows approaching 8000 m^3/s. This behavior is consistent with gravity-current (salt-wedge) dynamics, in which stratification, bottom roughness, and interfacial shear influence mixing and near-bed flow structure, thereby affecting sediment retention conditions [9–11]. These processes promote sediment deposition near the river mouth, where accumulations must be regularly removed through dredging to maintain navigability.

Despite sustained efforts to improve navigation, the intrinsic physical forces of the Magdalena River have posed persistent challenges. Attempts to maintain a deep, straight channel conflict with the river's inherent tendency toward sinuosity and, historically, toward a branched mouth with multiple islands. Nineteenth-century maps document the presence of such islands—some identified by name—connected to the Caribbean Sea and facilitating flow distribution at the mouth. This historical evidence highlights the persistence of multi-thread and island-forming tendencies, consistent with distributary behavior documented in large alluvial rivers and reported for the Magdalena mouth [12,13].

In parallel, a growing body of literature frames nature-based solutions (NBS) and "working-with-nature" approaches as strategies that harness geomorphic and ecological processes to achieve societal objectives with lower long-term maintenance and greater system robustness [14,15]. This perspective has been formalized in international guidance and policy frameworks (e.g., [14,16]), which emphasize alignment with natural system dynamics rather than structural overcontrol. In navigation contexts, this perspective translates into designs that (i) operate within morphodynamic constraints, (ii) enhance thalweg persistence, (iii) reduce chronic shoaling drivers, and (iv) minimize reliance on continuous dredging. Attempts to deepen a channel beyond its natural capacity inevitably alter the balance among liquid and solid discharge, sediment size, and driving slope, often leading to unintended morphodynamic responses consistent with documented adjustment mechanisms in sand-bed rivers [2,3].

However, documented applications of NBS explicitly targeting navigation reliability in large tropical sand-bed rivers remain comparatively scarce in the peer-reviewed literature, with most reported cases focusing on flood mitigation or ecological restoration rather than

navigation corridor stability. This gap motivates the process-based framework developed in the present study.

In alluvial channels, curvature generates secondary circulation that redistributes sediment and promotes deeper flow along the outer bank of bends, thereby enhancing thalweg persistence at the reach scale. Conversely, long low-curvature reaches tend to favor migrating bars and alternating shoals, which induce lateral thalweg oscillations and localized shallowing that are problematic for navigation. These tendencies depend on discharge variability, sediment characteristics, and channel geometry, and must therefore be evaluated within the specific context of the Magdalena River [4,17,18].

Nature-based solutions have thus gained relevance as an approach for addressing complex river management challenges by reconciling human needs with natural processes. The Magdalena River—also known as Kariguaña by Indigenous communities—provides a clear example where this perspective can be meaningfully applied.

At present, the Magdalena River faces a critical juncture. Continued deviation from its natural morphodynamic state risks triggering adverse economic, social, and environmental consequences. On one hand, the construction and maintenance of an artificially straight and deep navigation channel have proven unsustainable, given the persistent need for dredging and structural intervention. On the other hand, neglecting intrinsic river dynamics jeopardizes the stability of ecosystems and communities that depend on the river.

Applying nature-based solutions to the Magdalena implies not only respecting its sinuosity and natural morphology, but also recognizing the limits of its capacity for sediment transport and navigation. Channel curvature promotes a stable and deeper thalweg through secondary-flow effects, whereas thalwegs in straight channels tend to be unstable, shifting laterally in response to bar dynamics. Adopting this approach has the potential to reduce maintenance costs while preserving essential ecosystem services. In this sense, the Magdalena could serve as a reference case for future river interventions, in which nature is no longer treated as an obstacle but as an ally in sustainable development.

This study provides a system-scale characterization of hydraulic, sedimentological, and morphodynamic conditions in the lower Magdalena River, with particular emphasis on the final kilometers upstream of the river mouth, where navigation constraints are most pronounced. The analysis is intended as a process-based diagnostic of the dominant controls on shoaling and thalweg instability, and as a foundation for the design of interventions consistent with NBS principles. Despite extensive project documentation related to the Magdalena navigation corridor, there remains limited peer-reviewed synthesis explicitly linking (i) river planform and bar dynamics, (ii) river–estuary exchange processes, including salinity intrusion, and (iii) NBS-oriented design logic focused on navigation reliability. This manuscript addresses that gap by integrating these elements into a coherent process framework and a conceptual design proposal.

Based on this diagnostic, we propose a concept design that replaces the long straight terminal reach with a gentle meander configured to enhance thalweg persistence and modify near-mouth hydrodynamics relevant to sediment management. The proposed curvature introduces controlled momentum reorientation and secondary-flow effects that may (i) enhance cross-sectional mixing and weaken persistent stratification in critical zones, and (ii) steer the main flow toward deeper offshore bathymetry, potentially improving sediment export efficiency. These mechanisms are presented as process-based hypotheses consistent with established river and estuarine dynamics. Their quantitative verification—through detailed hydrodynamic–morphodynamic modeling and/or targeted field campaigns—is identified as a priority for future work.

Accordingly, the objectives of this study are to: (1) synthesize the dominant hydraulic and sedimentological controls on navigation constraints in the final reach of the Magdalena

River; (2) evaluate indicators of planform-related thalweg stability in relation to local bar dynamics; (3) interpret the role of salinity intrusion and near-mouth stratification as contributors to shoaling; and (4) formulate a nature-based conceptual design that aligns navigation performance with river–estuary morphodynamic constraints

2. Materials and Methods

2.1. Study Area and River Mouth Characteristics

The Magdalena River, known ancestrally as the Kariguaña River, drains approximately 22% of Colombia's total area, equivalent to 257,400 km^2. This river system runs 1612 km from south to north, fed by its main tributary, the Cauca River. From its source in the Nudo de las Papas, where it collects water from the high mountains of the Andes, to its mouth in the Caribbean Sea, the river crosses a diversity of tropical climates and ecosystems, flowing between the Eastern and Central mountain ranges.

Along its course, the Magdalena crosses varied landscapes, such as the arid areas of the Tatacoa Desert in the south and tropical regions towards its middle course. Historically, the river was navigable as far as the port of Colombia. In the section near the city of Honda, the river receives water from the Ruiz and Tolima snow-capped mountains, continuing northward until it reaches the Momposina depression, where its largest tributary, the Cauca River, is located. However, the Cauca basin has undergone serious changes in recent decades, especially due to the construction of the Hidrohituango reservoir.

Before reaching the sea, the Magdalena interacts with other significant water systems, such as the Sierra Nevada de Santa Marta, which partially feeds the Ciénaga Grande de Santa Marta, an ecosystem critically affected by various human activities. Finally, the river flows into the Caribbean Sea through Bocas de Ceniza, its delta located near the city of Barranquilla. This delta, characterized by asymmetrical topographic margins, has a lower right margin that is prone to flooding, while the left margin is elevated and contains both natural and artificial effluents.

The section studied in this article covers the last 40 km of the Magdalena River, from the town of Malambo to its mouth at Bocas de Ceniza. The Calamar station, located 100 km from Bocas de Ceniza, plays a crucial role in the river's hydrology, as at this point 500 m^3/s of the flow is diverted to the Canal del Dique, which connects to the bay of Cartagena de Indias.

At Bocas de Ceniza (located at coordinates 11°06′23″ N–74°51′10″ W), the Magdalena ends its journey by discharging its waters into the Caribbean Sea. Figure 1 shows both the river basin and its mouth, with satellite topography provided by Airbus. This image shows the sections chosen for flow measurements.

https://doi.org/10.3390/hydrology13030080

Figure 1. Map of the Magdalena basin with place names and other data.

2.2. History of Hydraulic Works and Channel Training

Prior to the construction of hydraulic works, the mouth of the Magdalena River exhibited a lobate delta morphology characterized by multiple channels, islands, and shallow depths. This configuration resulted from the dominance of fluvial processes, high sediment loads, and the relatively low energy of the Caribbean Sea, consistent with classifications of fluvial-dominated deltas (Figure 2) [19–21]. Historical bathymetries and maps confirm the presence of a multi-branch delta that posed persistent navigational difficulties since colonial times.

Systematic channel training began at the end of the 19th century with the objective of increasing depth and stabilizing navigation by preventing deltaic branching. The first major intervention was implemented between 1919 and 1923 by Black, MacKeney & Stewart, consisting of the construction of two converging breakwaters that confined the flow into a straight and narrowed channel (Figure 3) [16,20]. This intervention marked the beginning of a long-term engineering strategy based on channel contraction to enhance sediment transport capacity and scour.

Subsequent interventions during the mid-20th century reinforced this approach through the extension of breakwaters, the construction of groynes, and additional contraction dikes (Figure 3) [17,20]. These works progressively reduced the channel width from approximately 880 m to about 500 m, leading to local increases in depth from roughly 9 m to more than 12 m (Figure 4) [20]. However, these gains were repeatedly accompanied by unintended morpho-dynamic responses, including bar formation, localized erosion, and structural instability.

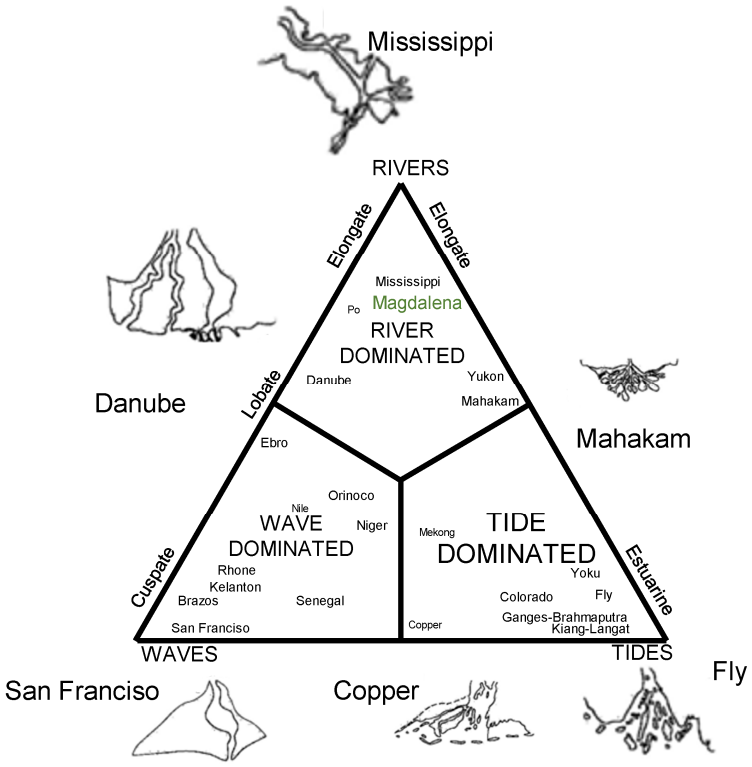

Figure 2. Classification of delta morphology according to the dominant processes [19].

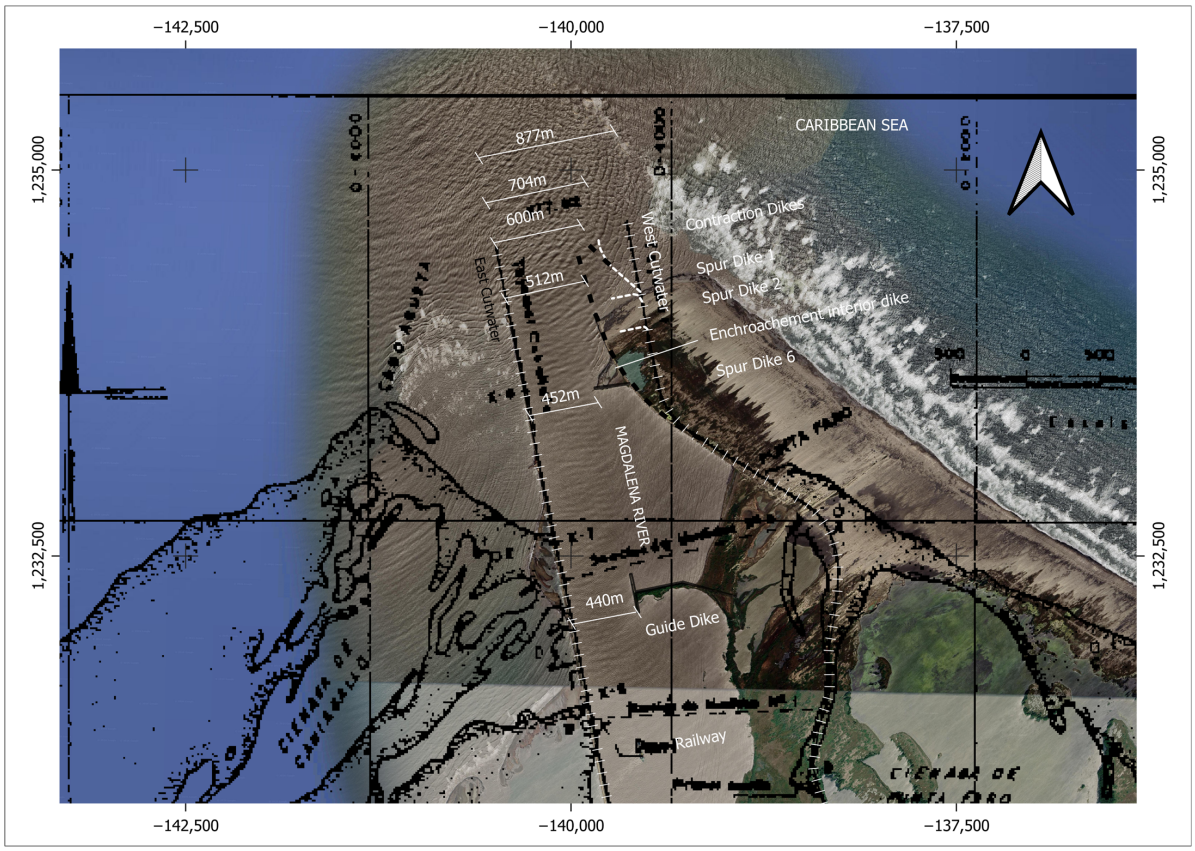

Figure 3. Overlapping plans of engineering interventions at the mouth of the Magdalena River: (a) Black, MacKeney & Stewart project (constructed in 1928) [20]; (b) Dent and Taylor project (1954 intervention) [20]; (c) later extension of the contraction dike to 704 m and construction of the inner dike, reducing the mouth width to 512 m [22]. The arrow indicates geographic north.

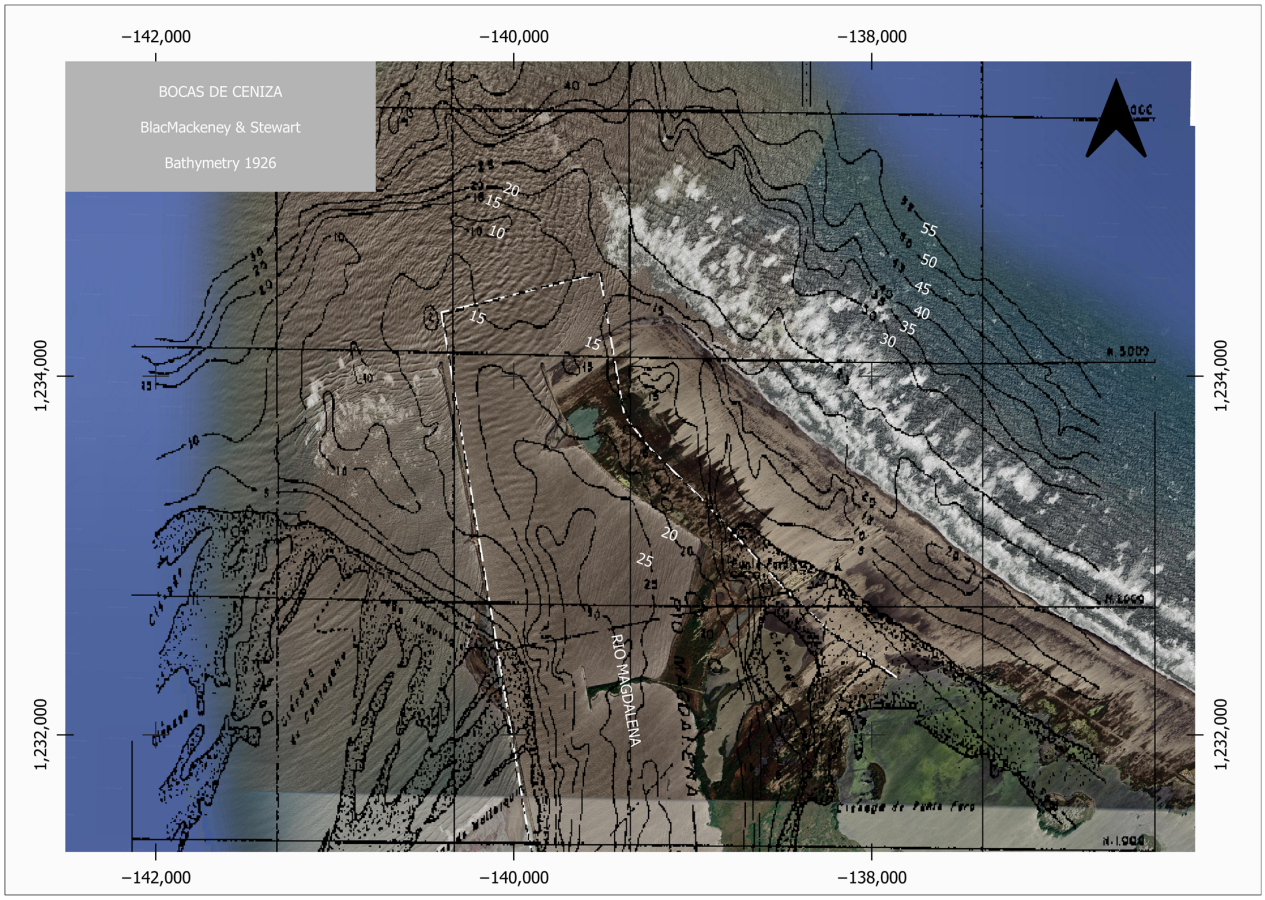

Figure 4. Bathymetry carried out at the mouth of the river before the construction of the first major work by Black Mackeney & Stewart [20]. Bathymetric contours are shown in feet (ft), consistent with the original survey data.

Several documented failures highlight the sensitivity of the system to excessive confinement. Collapses of both the western and eastern breakwaters in 1935 and 1945 coincided with rapid deepening and the development of unstable sediment accumulations near the river mouth [20]. These events were associated with gravitational instabilities and sediment mass movements toward the submarine canyon located offshore, a process recurrent in deepened river mouths [19,20,23].

Experimental studies carried out on physical scale models during the 1950s provided further insight into these processes. The studies demonstrated that the bar obstructing the river mouth is composed predominantly of fluvial sediment, with negligible contributions from marine currents or tides [20]. Although storm surges may reach several meters in height, their effect on river discharge and sediment transport was shown to be minor. These findings supported the continuation of channel narrowing as the primary engineering strategy, leading to additional contraction works during the 1960s that reduced the mouth width to approximately 512 m [20].

In the early 21st century, further training works were implemented, including spur dikes and closure dams designed to intensify flow concentration and minimize sedimentation within the navigation channel (Figure 5) [23–26]. These interventions resulted in a fully rectified and laterally confined channel over the final kilometers of the river, with widths locally reduced to less than 450 m. Although target depths close to 12 m have been achieved, regular dredging remains necessary to maintain navigability.

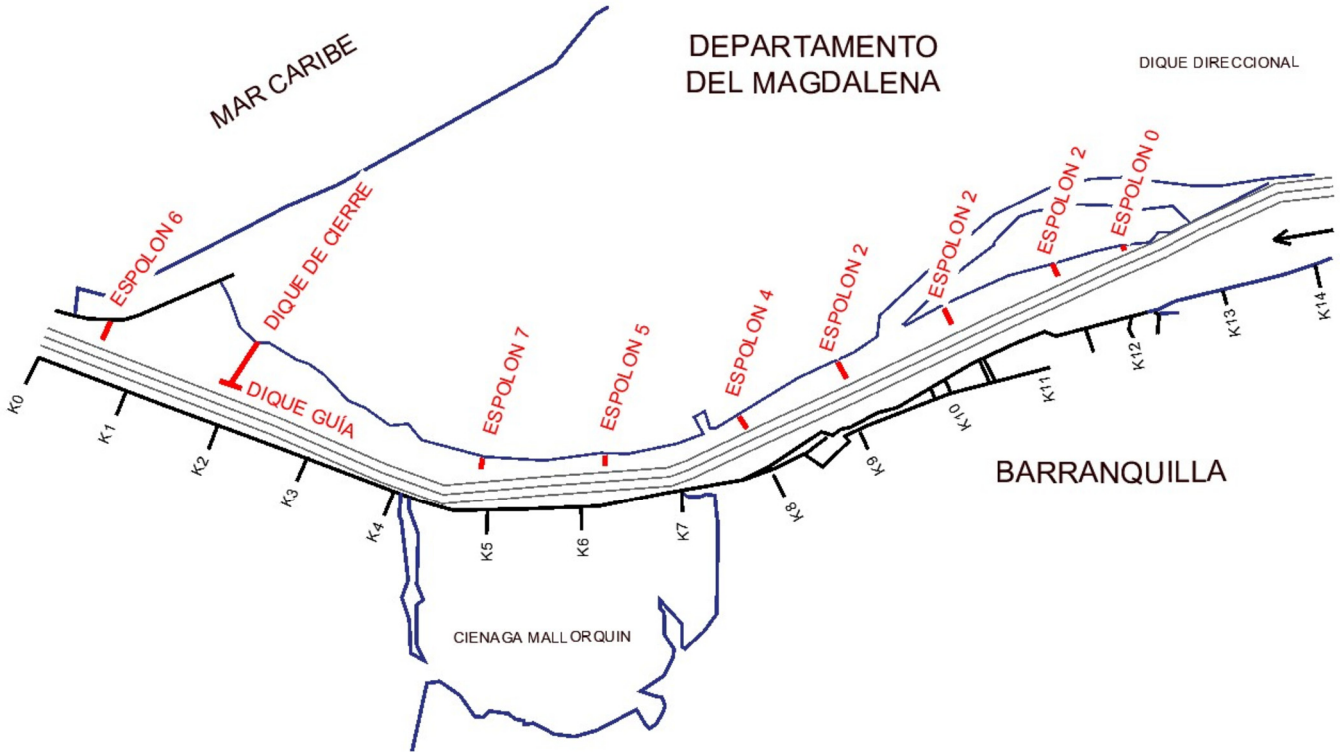

Figure 5. The state of the river is as shown by Moffatt & Nichol in this diagram. All the works designed between 2006 and 2008 can be seen.

Taken together, the historical evolution of hydraulic works at the Magdalena River mouth reveals a consistent pattern: channel narrowing can temporarily increase depth, but it also promotes instability, structural failure, and renewed sedimentation. Moreover, historical observations already noted the spontaneous tendency of the thalweg to develop curvature, with radii of several kilometers, reflecting the river's natural mechanism for energy dissipation and sediment redistribution. These documented processes provide a scientific basis for reconsidering planform geometry and for framing alternative interventions within a NBS perspective, grounded in the reproduction of geomorphic configurations that have proven dynamically stable over time.

2.3. Data Collection and Available Datasets

The study of the last 40 km of the Magdalena River included the evaluation of various hydrodynamic variables characteristic of this river system. To this end, six HOBOware Pro U20 level sensors, with an accuracy of 0.5 cm, were installed along this stretch. These devices recorded the water level every 15 min during the five months of the measurement program.

Three detailed bathymetric surveys were carried out with a resolution of 3 × 3 m:

First campaign: from 23 November to mid-December 2017.

Second campaign: 3 March to 24 April 2018.

Third campaign: 11 to 30 July 2018.

The objective of these campaigns was to record the conditions of the river during high, low, and medium water periods, respectively. However, in 2017, the flow did not exceed its average value, remaining almost constant throughout the wet season until its decline at the end of January. The average flow during these months was 7000 m^3/s, which allowed for stable bathymetry for that flow. In March, the flow reached its minimum and began to rise almost immediately, reaching 7000 m^3/s again in July.

Bathymetry was performed using a Reson 8101 multibeam echo sounder Reson Inc. USA, a Trimble SPS-461 GPS and gyroscope Trimble Heavy Civil Construction Division,

10368 Westmoor Drive Westminster, Colorado 80021, and an SMC IMU-108 motion sensor, SMC—Ship Motion Control, Estocolm Sweden. Data processing was carried out using PDS2000 software version 4.3.06 and a Valeport Monitor CTD sound velocity profiler both from Teledyne Marine Technologies Incorporated Daytona Beach USA, was used.

Along the 40 km studied, flow measurements were taken at 13 different sections using two devices: RiverRay and RiverPro. Liquid gauging was carried out monthly at these thirteen stations and, at six of them, solid flow was also measured. Figure 1 shows the position of the sections and points recorded.

Outside the main channel and around the mouth, wave and current data were recorded with a 1000 kHz AWAC device, in addition to salinity and suspended sediment measurements. Additionally, acoustic surveys and profiles of the subsoil were carried out, which allowed the identification of rock formations in the area.

3. Results

3.1. Hydrology Summary

The Barranquilla area can be defined as dry or very dry; without the constant flow of the Magdalena River, this region would be practically desert-like. According to average rainfall data and approximate calculations of potential evaporation using the Thornethwaite method, October is the only month in which precipitation exceeds evapotranspiration on average, as shown in Figure 6, although only by a few tens of millimeters. During the rest of the year, average evapotranspiration exceeds precipitation by approximately 100 mm/month, reaching values of around 130 mm/month in the first months of the year. In general terms, drought should be a constant condition in the area.

Fortunately, the Magdalena River is the main source of water for these lands. The aquifer is recharged during the winter months, between October and December, when the river carries a higher flow. The Magdalena constantly feeds the lateral marshes, except in summer, when the opposite phenomenon occurs and these marshes supply water to the river, with a reverse flow, approximately when the river flow is lesser than 5000 m^3/s [27]. However, pressure on the river is increasing due to the construction of new dams for hydroelectric power production and increased water use in the basin.

Reservoirs regulate maximum flows and create water bodies with large exposed surface areas, contributing both to increased evaporation and to a reduction in peak discharges, which are most conducive to the recharge of lateral aquifers. As a result, infiltration into the wetlands is expected to decline progressively, seriously affecting these ecosystems. The full effects of the most recent dams constructed in the Magdalena basin may not become evident for several years.

The wetlands surrounding the Magdalena are undergoing progressive drying, particularly the Ciénaga Grande de Santa Marta, which is showing signs of salinization as river inflow decreases. This ecosystem has approximately 35 km of shoreline along the Caribbean Sea, enabling the maintenance of a unique and highly valuable biotic system dominated by mangroves.

The gradient of peak and average flows shows a clear downward trend, with aver-age values between 1971 and 2025 shown in Figure 7a. An additional analysis was performed using the Innovative Trend Analysis (ITA) and the Rescaled Adjusted Partial Sums (RAPS) methods to detect potential trends and regime shifts in the discharge series.

ITA is a graphical, non-parametric method based on the comparison of two sub-series of equal length, allowing the identification of increasing or decreasing trends without strict statistical assumptions. The ITA was applied by dividing the discharge time series into two equal sub-series arranged in ascending order and plotting them against each other in a Cartesian coordinate system. Deviations from the 1:1 line indicate the presence and

direction of trends, allowing the identification of increasing or decreasing behavior in different flow quantiles without assuming data normality.

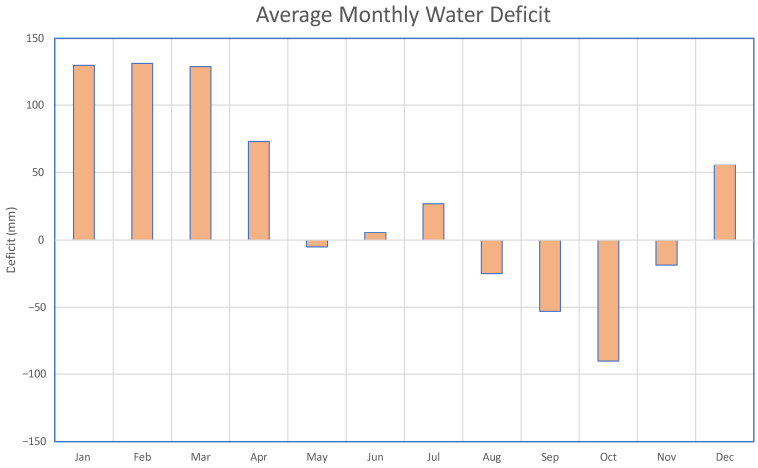

Figure 6. Difference between potential evaporation and average monthly precipitation (Evaporation-Precipitation), or monthly water deficit [28].

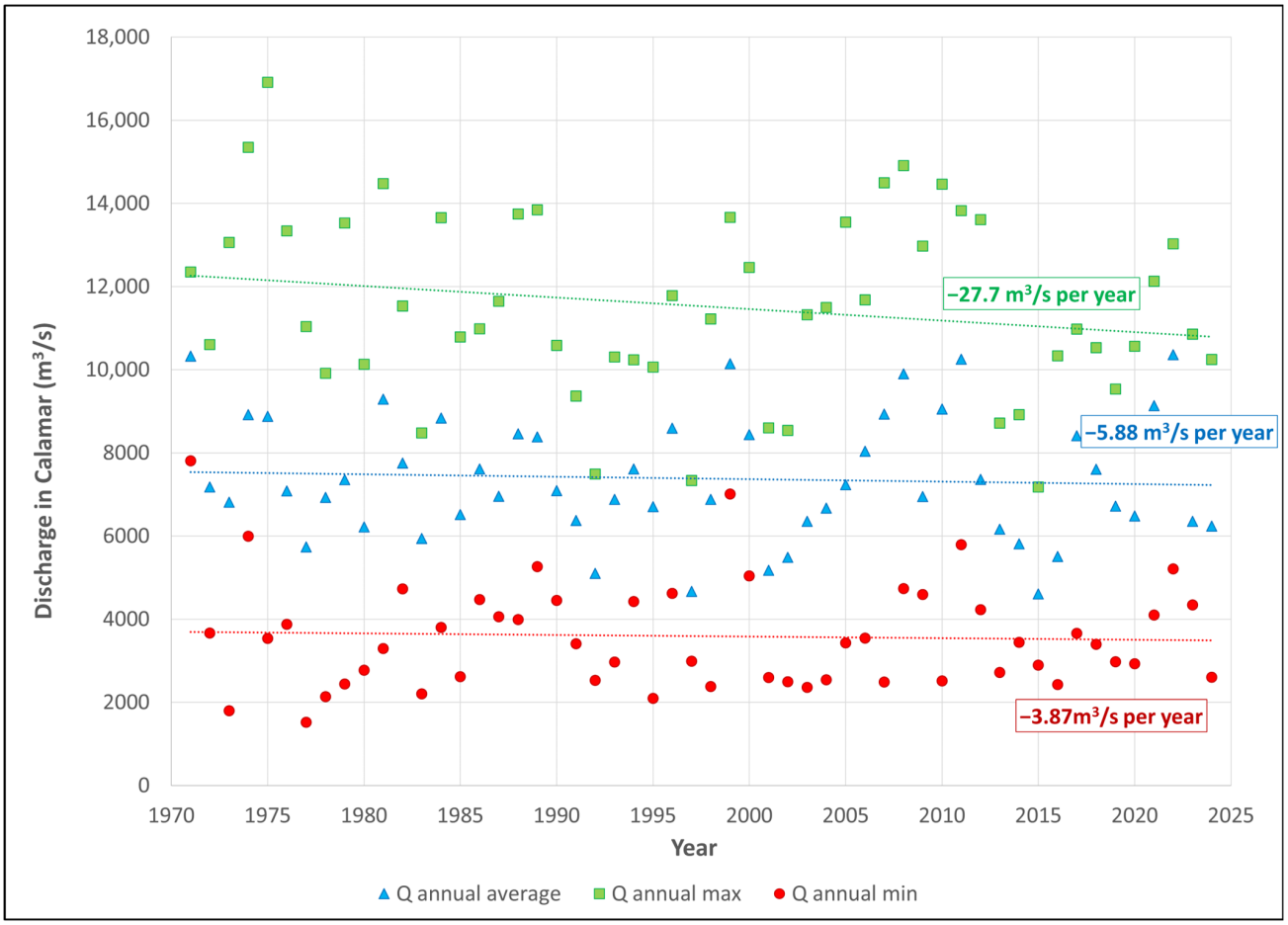

(a)

Figure 7. *Cont.*

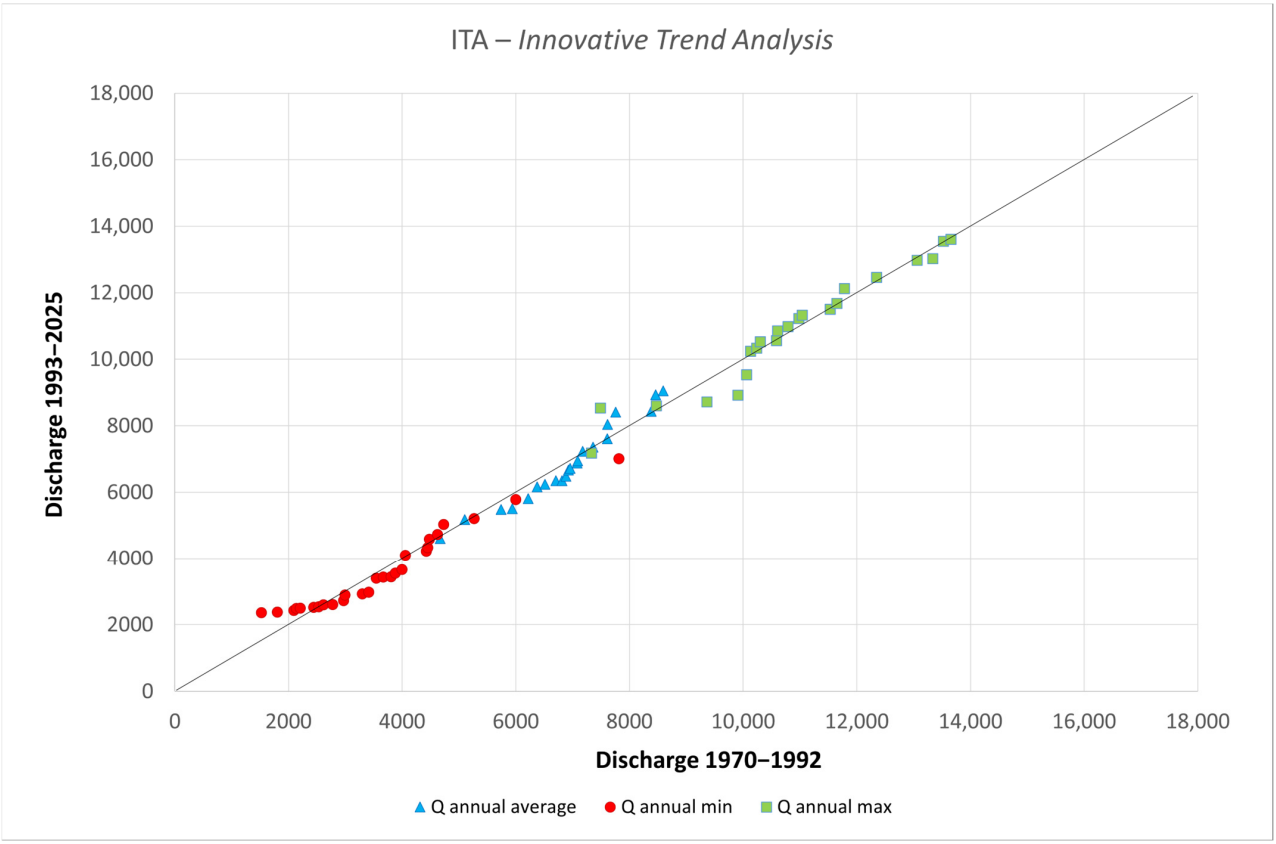

(**b**)

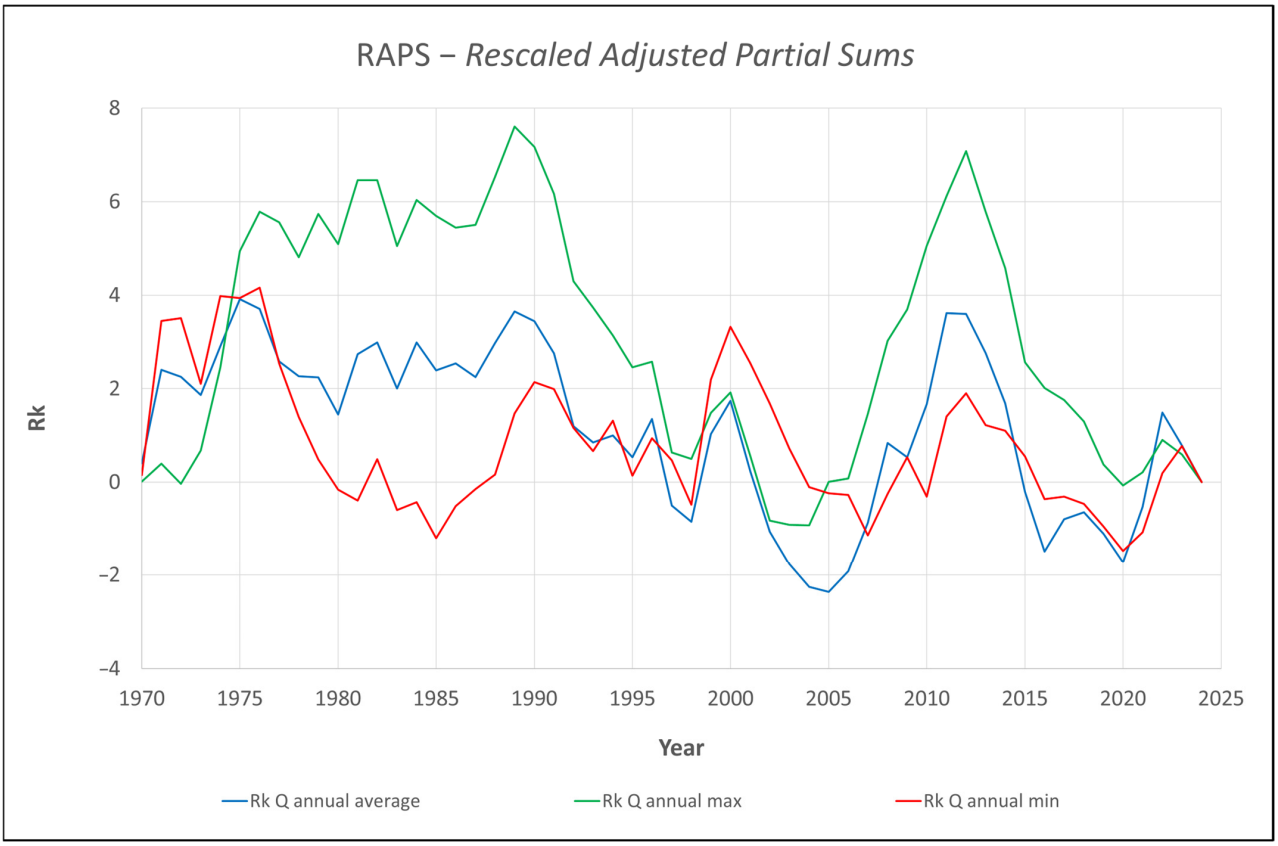

(**c**)

Figure 7. (**a**) Temporal evolution of maximum, average, and minimum flows of the Magdalena River at Calamar between 1971 and 2025. (**b**) Innovative Trend Analysis. (**c**) Rescaled Adjusted Partial Sums analysis.

RAPS is based on the cumulative summation of normalized deviations from the long-term mean and is particularly useful for identifying change points and shifts in the mean behavior of the series. Positive and negative cumulative departures indicate periods of above- and below-average conditions, respectively, while significant inflection points in the RAPS curve are interpreted as potential regime shifts in the hydrological series.

The ITA results (Figure 7b) indicate a general decreasing trend in river discharge, with the most pronounced decline observed in annual minimum flows. The RAPS analysis (Figure 7c) reveals a clear shift in the hydrological regime in the early 1990s, marking a transition from predominantly above-average to below-average discharge conditions.

Although part of the decline in minimum flows may be influenced by regulated ecological releases from reservoirs, the overall long-term trend remains downward.

Year after year, this pressure is leaving the riverbed drier. Both effects lead to a decrease in the amount of water that flows through infiltration into the surrounding land. Figure 8 shows four episodes of maximum rainfall that have occurred in recent decades: 1988, 1999, 2010, and 2011. The images show, with arrows, how water flows down the side slopes on either side of the riverbed. This obviously occurs during times of high water, which is why it is possible to see the water marks on the slopes towards the marshes, but it occurs at all times in the form of infiltration through the lateral sub-surface. The river regulation by dams will lead to fewer events like this with the obvious consequences.

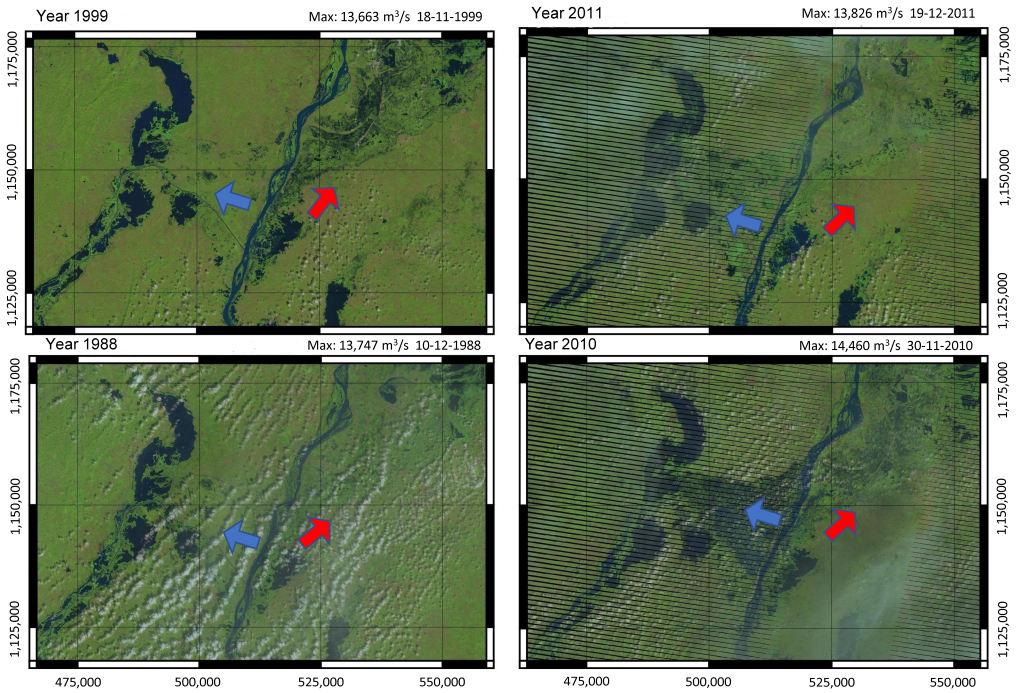

Figure 8. Lateral flooding during high water levels. Arrows indicates the surface lateral flow direction to the right (red) and left (blue) side of the river.

The Magdalena River has a gauging station in the town of Calamar, located 114 km from its mouth, where data has been recorded since 1940; however, only those considered most reliable since 1971 will be used. Downstream from this station, the river branches off into the Canal del Dique, a 110 km arm remodeled in the 1980s, which diverts a constant flow of approximately 500 m^3/s to the bay of Cartagena. An analysis of flow data from the last fifty years shows a decrease in water volume, precisely at the gauge before the fork. This continued reduction has negative effects on the functioning of the marshes surrounding the river, causing an increase in the frequency of flow exchange. The decrease in flow translates

into a lower dominant flow and shallower depths, which produces a morphological change in the riverbed, affecting the very use to which the river is being put: river navigation.

When comparing the flow measurements taken in the Barranquilla area with those taken at the gauging station itself, an interesting effect can be seen: the flow of the river upstream, in Calamar, is generally greater than downstream, showing a loss of flow along the riverbed. This loss of flow is due to the water that filters into the marshes. The filtration maintains its flow due to evaporation in the marshes and evapotranspiration in the surrounding land. Whenever the flow is above 4900 m^3/s, there is a loss of flow from Calamar to Barranquilla (see Figures 9 and 10), except for low flows, when the marsh also begins to feed the river through filtration. Figure 10 shows a comparison of the flow duration curve in Calamar and Barranquilla, where the point of intersection or exchange of flows between the marsh and the river can be observed. These exchanges have been less frequent in the past, but with each passing year, this reversal phenomenon occurs more frequently. In other words, the river's flow is reaching minimum levels more frequently [27], indicating that it is drying up more and more every day, and this is beginning to be noticed in the marshes, where salinity is increasing more frequently [28]. The explanation for the reversal is simple: when the river's flow is low, the driving slope of the channel is very low, all the more so because Manning's coefficient itself is lower. This lower slope means that the water level in the river, upstream of the mouth, begins to fall below the surrounding water table, a level that has been fed by the river's waters at times of high levels. This is when water flows from the marsh area into the riverbed, producing this change in flow values [29], which is observed comparatively between the data taken in Calamar and recorded near the mouth during the field campaign. The data are presented in Table 1.

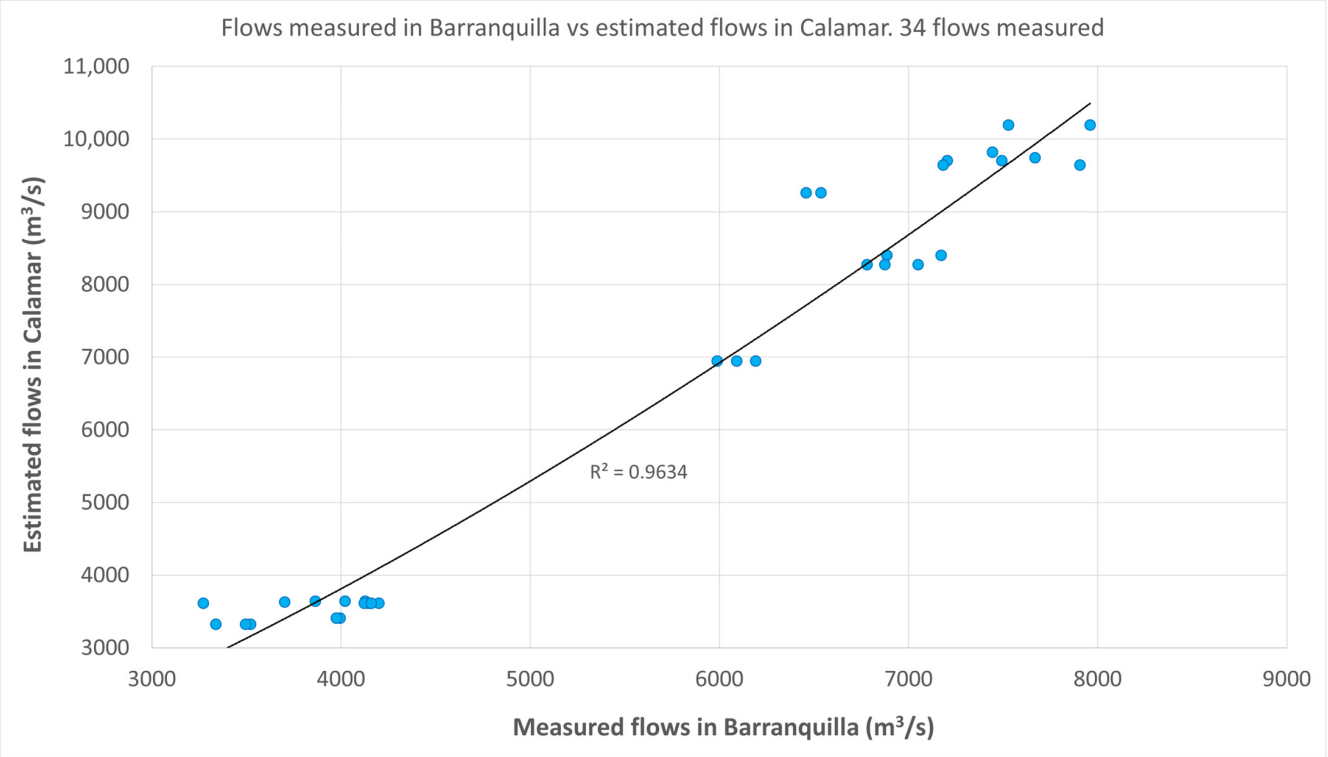

Figure 9. Gauging stations in Barranquilla compared with records in Calamar during the campaigns.

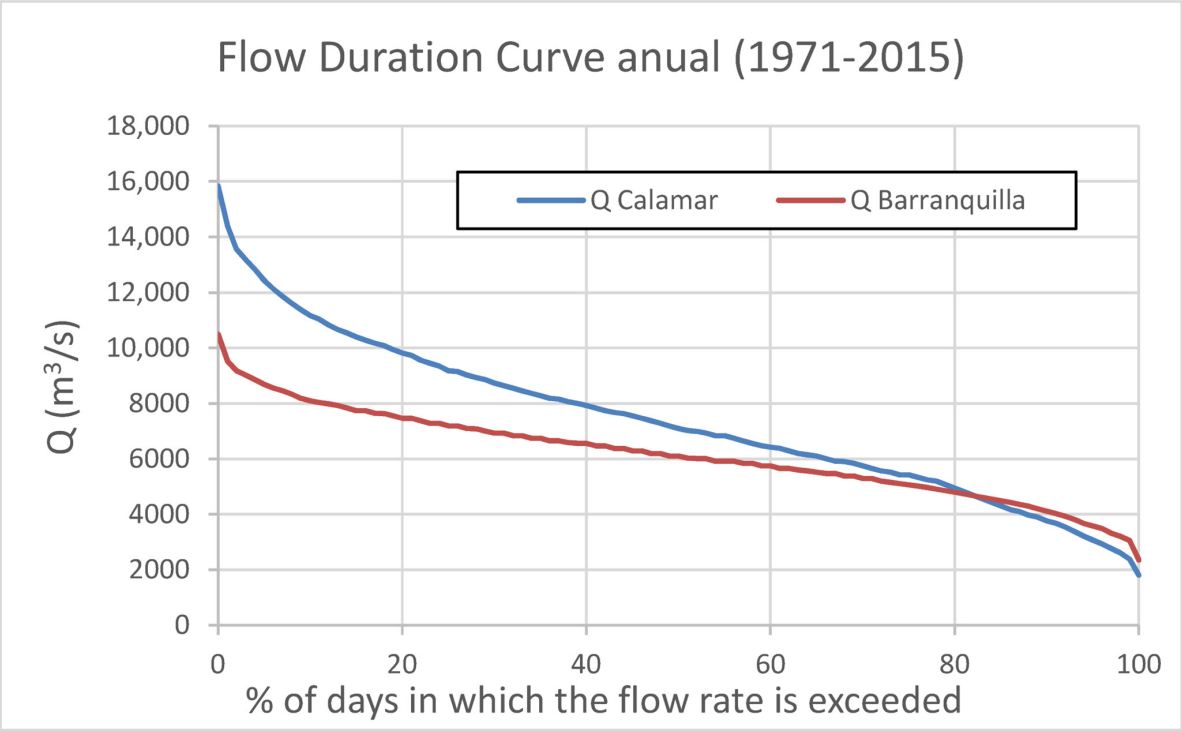

Figure 10. The FDC for Calamar and Barranquilla, the inflection point is above 5000 m^3/s.

Table 1. Records of the measured flow compared with the flow recorded in Calamar.

Station	Date	Width (m)	Depth (m)	Area (m^2)	Average Discharge (m^3/s)	Mean Velocity (m/s)	Level at Calamar (m a.s.l.)	Discharge Calamar (m^3/s)
1	7 November 2017	711	8	774	6459	1.1	6.6	9261
5	7 November 2017	669	11	694	6536	1.0	6.6	9261
6	7 November 2017	593	8	620	5327	1.2	6.6	9261
1	25 November 2017	739	17	6180	7205	1.2	6.8	9703
2	25 November 2017	544	19	6666	7493	1.1	6.8	9703
3	25 November 2017	709	9	5110	5567	1.1	6.8	9703
4	25 November 2017	496	8	2989	2673	0.9	6.8	9703
5	26 November 2017	642	20	7297	7668	1.1	6.8	9742
6	28 November 2017	578	10	5087	6562	1.3	6.9	9898
7	26 November 2017	558	15	5429	6703	1.2	6.8	9742
8	28 November 2017	374	13	2184	1783	0.8	6.9	9898
9	26 November 2017	259	12	2060	1763	0.9	6.8	9742
11	24 November 2017	566	17	6789	7906	1.2	6.8	9645
12	24 November 2017	521	18	5910	7183	1.2	6.8	9645
13	27 November 2017	686	22	6540	7443	1.1	6.9	9820
6 + 8	28 November 2017				8345			
1	19 December 2017	709	9	6307	7528	1.2	7.0	10,192
5	19 December 2017	645	11	7360	7959	1.3	7.0	10,192
6	19 December 2017	593	8	5057	6414	1.4	7.0	10,192
8	19 December 2017	375	6	2197	1843	0.9	7.0	10,192
6 + 8	19 December 2018				8257		7.0	10,192
1	23 January 2018	711	8	6554	6885	1.1	6.1	8401
5	23 January 2018	682	10	7384	7172	1.1	6.1	8401
6	1 February 2018	571	8	4615	5381	1.3	5.6	7556
8	23 January 2018	372	5	2082	1575	0.9	6.1	8401
6 + 8					6955			
1	23 March 2018	704	8	5390	3338	0.7	2.9	3325
5	23 March 2018	412	10	6228	3522	0.6	2.9	3325
6	23 March 2018	727	8	4260	2700	0.7	2.9	3325
8	23 March 2018	417	5	1539	795	0.6	2.9	3325
6 + 8	23 March 2108				3496		2.9	3325

The potential equation that fits the data in the graph at Figure 9 is given by the following expression.

$$Q_B = 14.73\ Q_C^{0.68} \quad (1)$$

where Q_B is the flow rate circulating through the city of Barranquilla and Q_C is the flow rate recorded in Calamar during the field campaign, which can be evaluated using an expression of the type

$$Q_C = 0.007\,h^2 + 9.20\,h \quad (2)$$

where h is the measurement at the gauging station in cm, the depth record ranges from approximately 200 to 900 cm, so the flow in Calamar would range between 2100 m^3/s and 14,000 m^3/s. Obviously, the records show values of 18,000 m^3/s measured at times of high water, but these values are uncertain because the water overflows the banks and are therefore very approximate [30].

3.2. Hydraulic and Sedimentological Characteristics of the Magdalena Riverbed

- Flows and Levels

Figure 11 shows the level records together with the flow values in Calamar and their estimate in Barranquilla, obtained during the field campaign. The level series show oscillations that reflect the influence of the tide; it can be noted that the data series closest to the sea, in Bocas de Ceniza (km 1), is short in time and its range of oscillation is approximately half a meter, corresponding to the natural tide of the Caribbean Sea in the area. The oscillations recorded in the probes located further upstream are smaller, decreasing as the distance from the sea increases; in Malambo (km 39), the level oscillations are only 15 cm. The water level also increases proportionally to the distance from the sea and the recorded flow.

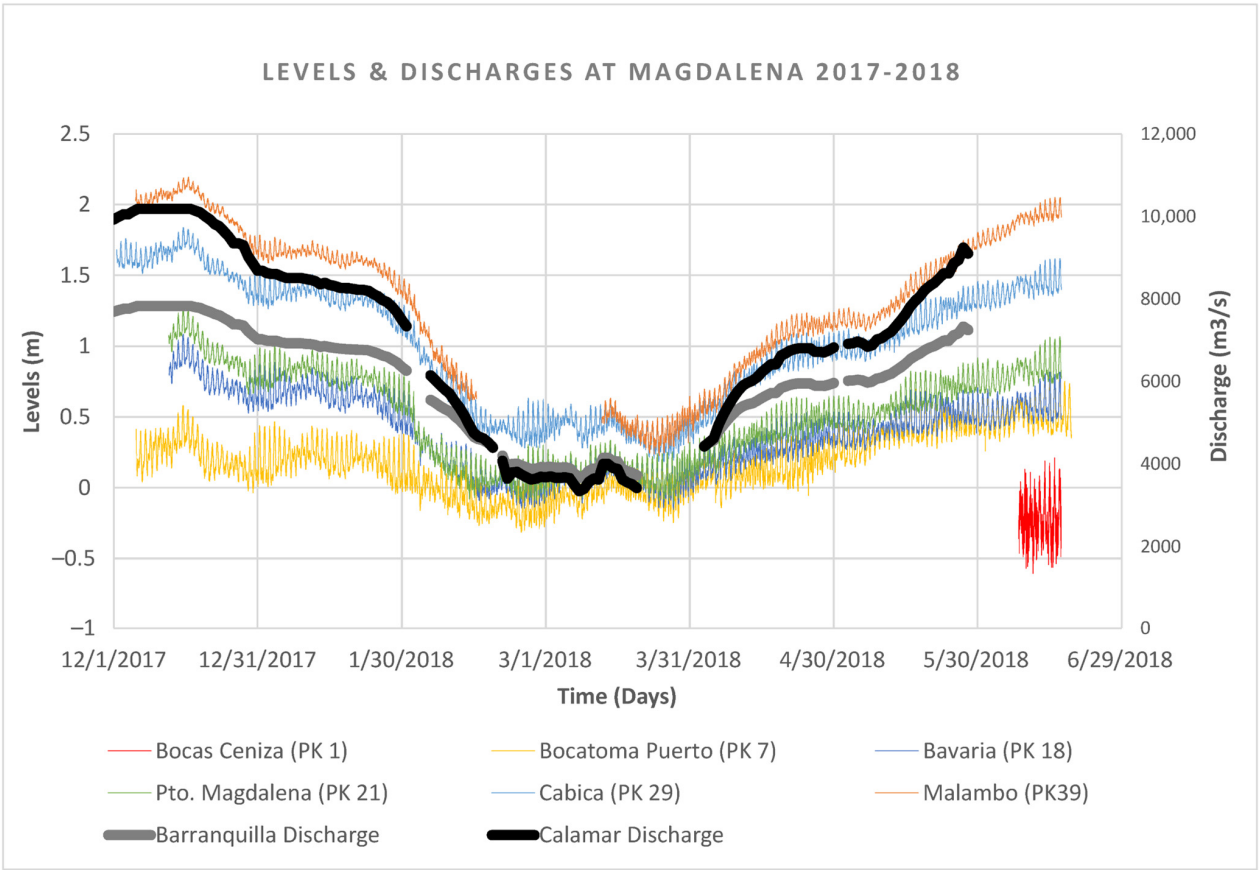

Figure 11. Relationship between levels and flows in the last 40 km of the riverbed.

The same Figure 11 shows the flows in Calamar and their estimate in Barranquilla, whose values can be read on the vertical scale on the right in m^3/s. It is interesting to note that, in

general, the flow in Calamar is greater than in Barranquilla, indicating a loss of water along the stretch. However, this behavior changes when flows are low; in this case, the flows in Barranquilla are higher than in Calamar. The Magdalena River, in the area between Calamar and the mouth, has several swamps that are fed by water from the river through filtration; otherwise, they would not exist, given the low rainfall in the area and high evapotranspiration. However, the collateral marshes are present; their area grows and shrinks depending on the time of year, indicating that there is a constant flow of water from the river to the marsh, and in some periods, the flow is reversed, feeding the river from the marsh.

This reversal of flows is explained by the transfer of water flow between the river and the surrounding aquifer, which gives rise to the marshes that make up the river's lateral landscape. When the flow is high, the energy gradient and water level in the river are high; therefore, as can be seen in the graph, for high flows the driving gradient is steep and the water levels are high. In this case, part of the river flow easily passes into the marshes, increasing the volume in the aquifer, not necessarily through surface flow, although this can also occur. This process decreases the flow in the river as it approaches the sea.

However, during periods of drought, the energy gradients and water level drop to minimum values, as can be seen in the same Figure 11 in the central part. All water levels in the probes tend to equalize, presenting very low driving gradients. River levels can fall below those of the aquifer, at which point the aquifer itself transfers water to the river; therefore, under these conditions, the flow in Barranquilla increases relative to Calamar. This reversal process during droughts was rare in the past; however, its frequency has been increasing, indicating drastic changes in the Magdalena basin [29].

First, the driving slope was evaluated for the different flows recorded at the Barranquilla station. To do this, the day of the flow was correlated with the date and time of the levels recorded. The average slope was divided into four sections, as shown in Figure 12. The first section, downstream, extends from Bavaria to Boca Toma del Puerto. The two intermediate sections include the right branch between Bavaria and Portmagdalena (just below the Pumarejo bridge old and new) and from this last point to downstream of Cabica Island. The last section extends from Cabica Island to Malambo.

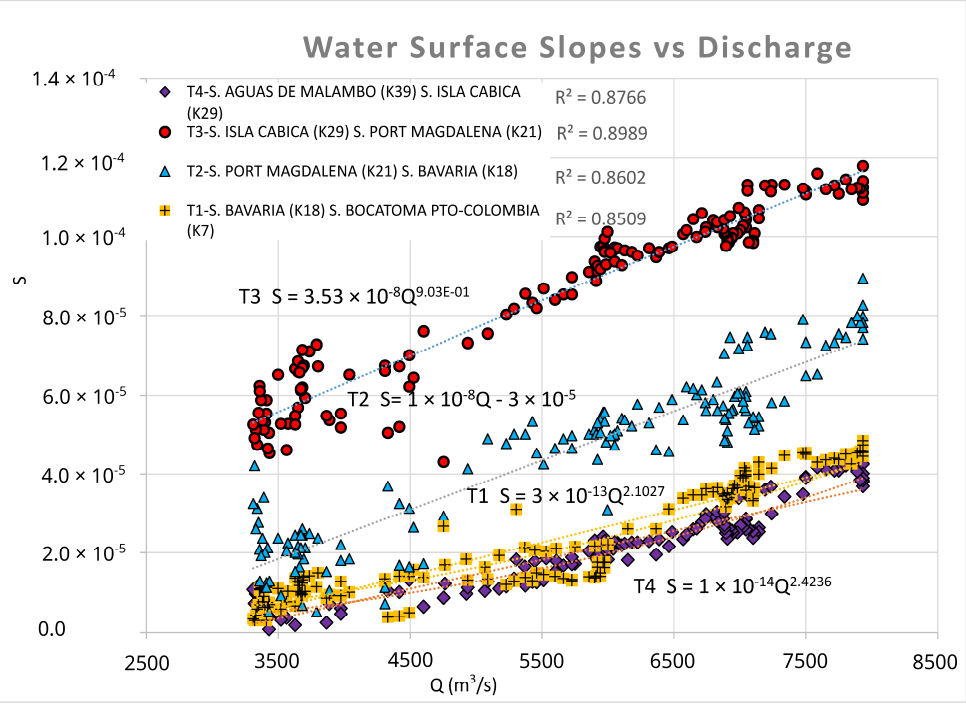

Figure 12. Driving gradients recorded on the Magdalena River.

It is interesting to note that the two intermediate sections, which cross the port area, have higher average slopes. It is also important to note that the slopes in the downstream and upstream reaches, which are in principle more natural, have approximately the same driving slopes. These driving slopes will be used for general hydrodynamic analyses as natural sections.

- Solid Transport and Flow Resistance

Measurement Results

During field tests, measurements were taken of the sediment concentration of several vertical profiles across various sections of the channel, together with the channel's flow measurement. In addition, the water level was recorded simultaneously during the experiments. Table 2 presents the data on the average geometric characteristics of the section: average depth H_{med}, section width B, and wet area of the section A, driving slope S_f measured with sensors on the date of the test, and flow measured during the campaign. The driving slope has been approximated with the water surface slope, as the influence of velocity energy is minimal. The last two columns of the table show Manning's flow resistance coefficient and the total solid flow in Kton/day. Stations 3 and 4 are located on the arms of Cabica Island, and stations 6 and 8 are located on the arms of Rondón Island. The solid flow recorded during those days in the different sections is practically constant, with a value of 2000 Kton/day. This can be verified by the sum of the solid flows in the arms. The average liquid flow on those days was 7200 m^3/s for a 0.12% sediment concentration.

Table 2. Assessment of total solid flow and Manning's resistance coefficient based on recorded data.

Station	Date	Mean Height (m)	Width (m)	Area (m^2)	Mean Discharge (m^3/s)	Mean Velocity (m/s)	Sf	n	Qs (Kton/Day)	Qs (Kton/Day)
1	25 November 2017	8.35	740	6180	6989	1.13	3.00×10^{-5}	0.020	2000	1648
2	25 November 2017			6666	7269	1.09	3.00×10^{-5}			
3	25 November 2017	7.15	715	5110	5400	1.06	1.10×10^{-4}	0.036	1411	1281
4	25 November 2017	5.98	500	2989	2593	0.87	8.80×10^{-5}	0.035	681	633
5	26 November 2017			7297	7438	1.02	8.00×10^{-5}			
6	28 November 2017	8.77	580	5087	6365	1.25	6.00×10^{-5}	0.025	557	557
7	26 November 2017			5429	6502	1.20	6.00×10^{-5}			
8	28 November 2017	5.75	380	2184	1730	0.79	6.00×10^{-5}	0.029	1586	1586
9	26 November 2017			2060	1710	0.83	6.00×10^{-5}			
11	24 November 2017	11.91	570	6789	7669	1.13	4.00×10^{-5}	0.028	2188	1846
12	24 November 2017	11.26	525	5910	6968	1.18	4.00×10^{-5}	0.025	1984	1697
13	27 November 2017	14.53	450	6540	7220	1.10	4.00×10^{-5}	0.032		1577

The situation of the Magdalena River is located in the dimensionless graphs of the regime theory presented in [31], in Figure 13. It is interesting to note that the Magdalena data collected in the field campaign agree quite well with the other channels. The dominant or formative flow value, 7400 m^3/s, has been used as the full channel flow for the calculations. Thus, the dimensionless flow value is defined as $\hat{Q} = Q/\sqrt{gD_{50}}D_{50}^2$, the dimensionless width as $\hat{B} = B/D_{50}$, and the dimensionless depth as $\hat{H} = H/D_{50}$. The variable that deviates most from the trend is the average bed slope, as can be seen in the same figure.

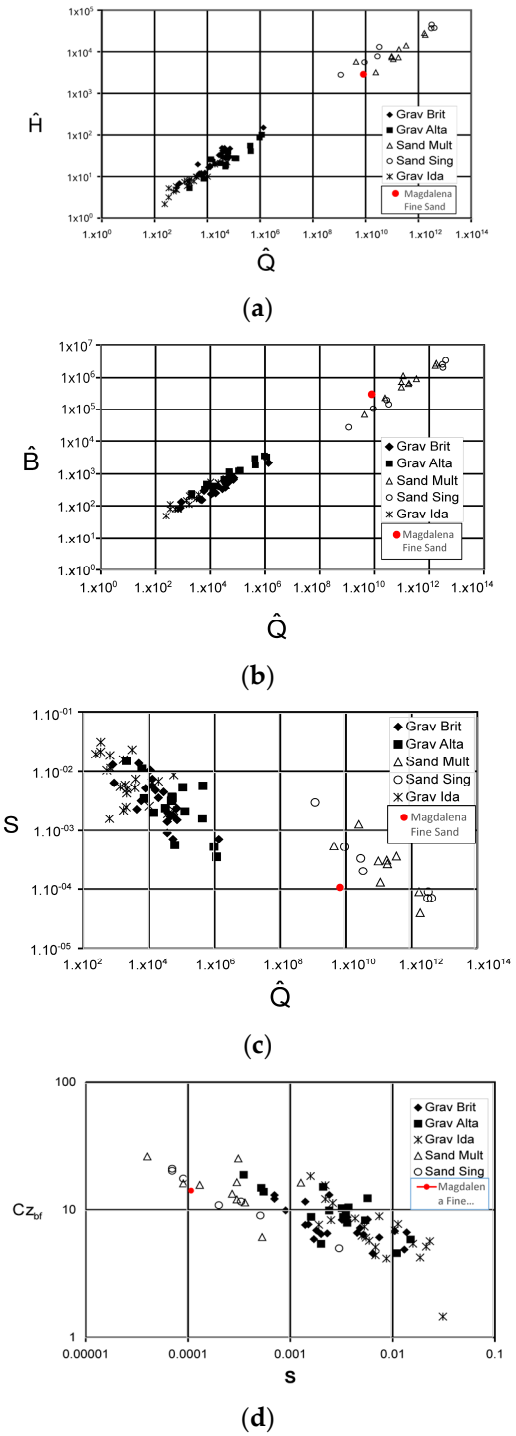

Figure 13. The Magdalena River dimensionless variables in the dimensionless graphics provided by ch3 Parker. (**a**) dimensionless width vs. dimensionless discharge, (**b**) Dimensionless Height H vs. Q; (**c**) Slope S vs. Q; (**d**) Chezi Cz vs. S.

- Assessment of the Solid Background Flow, Suspension, and Flow Resistance

The flow resistance coefficient was evaluated based on the driving gradients recorded along the 40 km. Several sections were used, and two sections are presented as examples: S02 and S11. Their position on straight sections is ideal for calculation, although, as will be seen, S02 has the typical curvature of the river area. For its evaluation, the methodology presented by [32], was used, in which Einstein's stress decomposition is used. In this methodology, the total stress $\overline{\tau}_o$ is defined as the sum of the skin stresses $\overline{\tau}_s$ and shape

stresses $\overline{\tau}_f$, such that: $\overline{\tau}_o = \overline{\tau}_s + \overline{\tau}_f$. The section was divided into vertical strips, so that the liquid flow, solid flow, and suspended flow could be evaluated in each one. The bottom solid flow rate is evaluated based on the assessment of skin stresses according to Einstein's decomposition. The suspended flow rate of the bed material is evaluated based on the drag formulation of [33], performing the integral of the Rouse profile for each flow strip, such that:

$$q_{ss} = \frac{u_* EH}{\kappa} \int_{\zeta_b}^{1} \left[\frac{(1-\zeta)/\zeta}{(1-\zeta_b)/\zeta_b} \right]^{\frac{v_s}{\kappa u_*}} \ell n\left(30\frac{H}{k_c}\zeta\right) d\zeta \tag{3}$$

where entrainment can be evaluated with:

$$E = \frac{AZ_u^5}{1 + \frac{A}{0.3}Z_u^5} \tag{4}$$

where q_{ss} is the unit solid flow in suspension, E is the sediment drag, $A = 5 \times 10^{-7}$, ζ is the percentage of depth where it is evaluated, ζ_b the percentage of depth where the concentration profile begins, κ Von Karman's universal constant, u_* shear velocity, v_s falling velocity in water of a particle of size D_{50}, $k_c = 11H/e^{(kC_z)}$, H depth of the analyzed fluid strip, $C_Z = U/u_*$, u_{*s} skin shear velocity, U average velocity, $Z_u = Re_p^{0.6} S^{0.07} u_{*s}/v_s$, $Re_p = \sqrt{gRD_{50}} D_{50}/v$ is the particle Reynolds number, $R = (\rho_s/\rho - 1)$ relative submerged specific weight, ρ_s and ρ density of sediment and water, respectively, and v the kinematic viscosity of water. The transport equation used in this modeling was Ashida Mishiue, as proposed by Parker [31],

$$q_b = \sqrt{RgD_{50}} D_{50} (\overline{\tau}_s{}^* - 0.05)\left(\sqrt{\overline{\tau}_s{}^*} - \sqrt{0.05}\right)$$

where $\overline{\tau}_s{}^*$ is the dimensionless skin stress or Shields parameter and g the gravity acceleration.

Applying this methodology, the following magnitudes are obtained: bottom solid flow, suspended solid flow, and flow resistance coefficient. Table 3a presents the results for section S02, while Table 3b summarizes the corresponding results for section S11. The data for December 2017 were analyzed, taking advantage of the fact that the flow remained almost constant for several weeks, ensuring a stable and consistent hydraulic state between all measurements.

3.3. Driving Slope and Flow Resistance

The method uses the driving slope measured for the average flow as its starting parameter. In many cases, this complicates the calculations due to the difficulty of measuring the driving slope (approximately the slope of the water surface) in situ at the time of gauging. Fortunately, in this study, water levels were measured with good accuracy over time at six points along the channel, which made it possible to determine the driving slope continuously over time in the different sections. As for the average sediment size, the median sediment size (D_{50}) is 0.2 mm and the median sediment size (D_{50}) is 0.455 mm. The kinematic viscosity of water ($1. \times 10^{-6} m^2/s$) and n_k of 2.5 were used, since ks is of the order of $n_k D_{s90}$. Section S02 has some curvature, and the calculated resistance coefficient varies between 0.012 and 0.035, which is a significant variation and reflects the importance of taking this variation into account in all calculations for a channel in general. Section S11 is located on a fairly straight stretch, and Table 3 shows that the Manning coefficient varies from 0.012 for low flows to 0.036 for high flows. The variation in the coefficient can only be partially explained by the formation of bottom shapes.

Table 3. (**a**) Computed hydraulic and sediment transport parameters at section S02. (**b**) Computed hydraulic and sediment transport parameters at section S11.

(a)														
Hmax	**B**	**P**	**Rh**	**Sf** $\times 10^{-6}$	**A**	**Q**	**Qsb**	**Qss**	**Qsb**	**Qss**	**Qstp**	**Cv**	**n**	**Fr (−)**
	(m)				**(m^2)**		**(m^3/s)**			**(Kton/day)**				
15.5	516	519	9.9	1.1	5141	2395	1.76×10^{-7}	4.50×10^{-5}	0	0	0	0.0%	0.010	0.047
16.0	522	524	10.3	2.4	5401	3044	6.60×10^{-5}	3.00×10^{-4}	0	0	0	0.0%	0.013	0.056
16.5	523	526	10.8	5.1	5662	3371	2.41×10^{-4}	1.22×10^{-3}	0	0	0	0.0%	0.018	0.058
17.0	524	528	11.2	10.4	5923	3933	8.39×10^{-4}	7.09×10^{-3}	0	2	2	0.0%	0.024	0.063
17.2	524	528	11.4	13.8	6028	4244	1.36×10^{-3}	1.57×10^{-2}	0	4	4	0.0%	0.027	0.067
17.4	525	529	11.6	18.2	6133	4670	2.23×10^{-3}	3.69×10^{-2}	1	8	9	0.0%	0.029	0.071
17.6	525	530	11.8	24.0	6238	5187	3.64×10^{-3}	9.03×10^{-2}	1	21	22	0.0%	0.030	0.077
17.8	526	530	12.0	31.5	6343	5839	5.95×10^{-3}	2.31×10^{-1}	1	53	54	0.0%	0.032	0.085
18.0	526	531	12.1	41.3	6448	6642	9.71×10^{-3}	6.11×10^{-1}	2	140	142	0.1%	0.033	0.094
18.2	527	532	12.3	53.9	6554	7622	1.58×10^{-2}	$1.65 \times 10^{+0}$	4	378	382	0.2%	0.034	0.106
18.4	527	532	12.5	70.1	6659	8808	2.57×10^{-2}	$4.53 \times 10^{+0}$	6	1037	1043	0.5%	0.034	0.119
18.6	527	533	12.7	91.0	6764	10,234	4.15×10^{-2}	$1.24 \times 10^{+1}$	9	2851	2860	1.2%	0.034	0.136
18.8	528	534	12.9	117.9	6870	11,937	6.67×10^{-2}	$3.39 \times 10^{+1}$	15	7757	7772	2.8%	0.034	0.155
19.0	528	534	13.1	152.1	6975	13,962	1.07×10^{-1}	$8.96 \times 10^{+1}$	24	20,512	20,537	6.4%	0.034	0.177
19.2	529	535	13.2	195.9	7081	16,358	1.69×10^{-1}	$2.24 \times 10^{+2}$	39	51,300	51,338	13.7%	0.034	0.203
(b)														
Hmax	**B**	**P**	**Rh**	**Sf** $\times 10^{-6}$	**A**	**Q**	**Qsb**	**Qss**	**Qsb**	**Qss**	**Qstp**	**Cv**	**n**	**Fr (−)**
	(m)				**(m^2)**		**(m^3/s)**			**(Kton/day)**				
11.0	531	534	8.8	1.9	4683	2234	0	1.90×10^{-5}	0	0	0	0.0%	0.012	0.051
12.0	535	539	9.7	4.7	5216	3501	2.19×10^{-4}	3.03×10^{-4}	0	0	0	0.0%	0.015	0.069
13.0	538	543	10.6	11.0	5752	4148	9.28×10^{-4}	1.61×10^{-3}	0	0	1	0.0%	0.022	0.071
14.0	542	547	11.5	23.9	6293	5408	3.75×10^{-3}	1.51×10^{-2}	1	3	4	0.0%	0.029	0.081
14.5	543	549	12.0	34.5	6564	6386	7.40×10^{-3}	5.43×10^{-2}	2	12	14	0.0%	0.032	0.090
15.0	544	551	12.4	49.3	6836	7690	1.44×10^{-2}	2.09×10^{-1}	3	48	51	0.0%	0.033	0.102
15.2	545	551	12.6	56.6	6944	8317	1.88×10^{-2}	3.62×10^{-1}	4	83	87	0.0%	0.034	0.108
15.4	545	552	12.8	65.0	7053	9013	2.44×10^{-2}	6.30×10^{-1}	6	144	150	0.1%	0.034	0.114
15.6	545	553	13.0	74.4	7162	9783	3.15×10^{-2}	1.1	7	252	259	0.1%	0.035	0.121
15.8	546	553	13.1	85.1	7271	10,633	4.07×10^{-2}	1.92	9	439	448	0.2%	0.035	0.129
16.0	546	554	13.3	97.1	7381	11,569	5.24×10^{-2}	3.34	12	766	778	0.3%	0.035	0.137
16.2	547	555	13.5	110.6	7490	12,597	6.72×10^{-2}	5.82	15	1331	1347	0.5%	0.035	0.146
16.4	547	555	13.7	125.8	7599	13,725	8.60×10^{-2}	$5.82 \times 10^{+1}$	20	2306	2325	0.7%	0.036	0.156
16.6	548	556	13.9	142.9	7709	14,959	1.10×10^{-1}	$5.82 \times 10^{+2}$	25	3970	3995	1.2%	0.036	0.166
16.8	548	557	14.0	162.0	7819	16,308	1.39×10^{-1}	$5.82 \times 10^{+3}$	32	6784	6816	1.8%	0.036	0.178

Figure 14 shows the velocity profiles obtained at different verticals; each of them represents the horizontal average of a series of profiles measured with the ADCP profiler. The equation governing these profiles, $\frac{u(z)}{u_*} = \frac{1}{k} ln\left(\frac{30z}{k_s}\right)$, allows the logarithmic slope to be identified, which is expected to be close to 0.41; however, the results obtained show a significant deviation from this value. In particular, the profiles associated with a flow rate of 7400 m^3/s (shown in gray) correspond to a von Kármán coefficient value of k = 0.25, while for flow rates below 3400 m^3/s the value is reduced to k = 0.10. It is interesting to note that the value of k is lower when the discharge is smaller and the bed is nearly flat. This suggests that the change in Manning's coefficient may be due to another phenomenon, rather than to the presence of bedforms. This same trend is shown in [34].

This notable variation is associated with the influence of the concentration of suspended sediment in the area near the bed, where the concentration of particles is very high and directly affects the production of turbulent energy. The phenomenon is significant enough to be addressed in depth in a separate study.

The distance to the axis that marks the intersection point of the velocity profile with the ordinate axis represents that $k_s = \frac{30h}{e^d}$, where d is that distance and d is the average depth of the flow in the area. It can be seen that the intersection points with the ordinates are similar for both the steeper and gentler slopes. Although they are not identical, the differences are not substantial, suggesting that k_s is comparable in both cases. In fact, the gentler slopes intersect at lower values than the steeper slopes where the flow was greater.

Table 2 shows that at the end of 2017, the flow of the Magdalena River remained fairly stable near the dominant flow, estimated at 7400 m^3/s. According to measurements, this

flow is transporting approximately 2000 KTon/d of sediment, which is roughly the same in all recorded sections. On the other hand, in Table 3, it is estimated that the transport of bottom sediment plus suspension is in the order of 382 and 51 Kton/d in sections S02 and S11, respectively. This is in the order of 20% and 2.6%, respectively. As can be seen, these amounts are a significant percentage of the total evaluated. These findings suggest that section S02 is mobilizing more sediment than S11 [35].

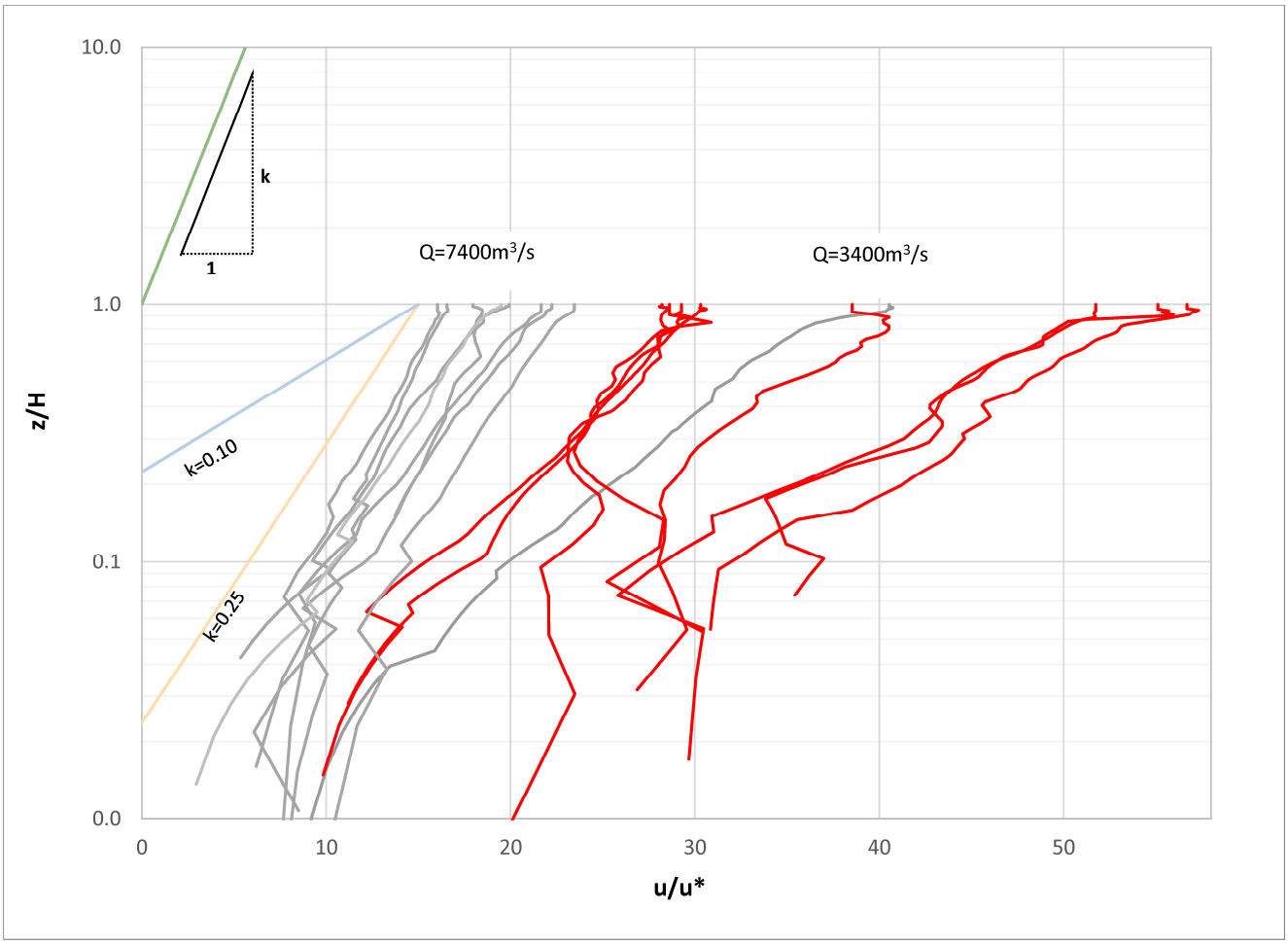

Figure 14. Velocity distribution at two different times, for high and low flows. Gray indicates high flows and red low flows.

Figure 15a,b show that section S11 is wider and shallower, however, it can be observed that the flow capacity is similar. The big difference between these two sections is in the curvature. S02 has the natural curvature of the river, with values close to a 5000 m radius of curvature, while S11 is in a straight area of anthropogenic origin, due to the dikes that were placed, as can be seen in the latest modification carried out in the Magdalena riverbed (see Figure 5). The curvature generates a force that the outer bank of the channel exerts on the water, forcing the flow to change direction. If the flow maintains approximately the same geometry and momentum flow between one section and the next, the force exerted by the bank generates a helical flow, so that the water in contact with the surface generates much greater stresses than if the flow continued straight. These additional stresses exerted by the helical flow generate greater depths in the channel, with a more stable Thalweg over time. Figure 15c shows that the hydraulic capacity is nearly the same.

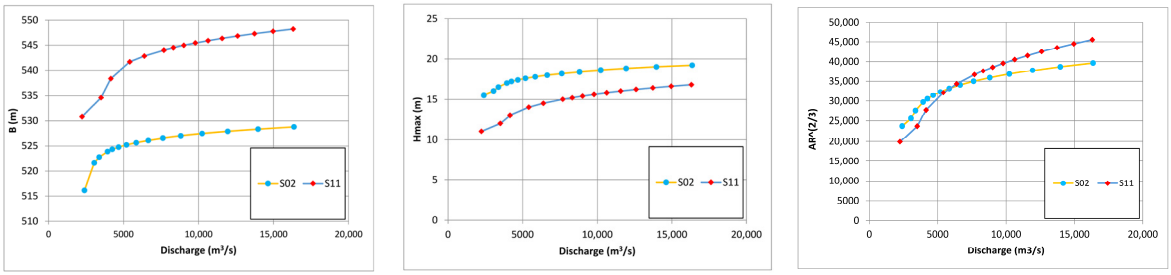

(**a**) (**b**) (**c**)

Figure 15. Comparison between sections S02 and S11: (**a**) width–discharge relationship; (**b**) depth–discharge relationship; and (**c**) hydraulic conveyance capacity.

Regarding solid transport, Figure 16 shows the evolution of the calculated solid transport in its different ways in sections S02 an S11 with increasing discharge. Compared with the data points in the graph representing total measured sediment discharge, they are lower values. The total discharge measured was 2000 kton/d. The approximate flow rate for sections S02 and S11 is 3 to 4 kTon/d for bed sediment and 378 and 48 kTon/d for suspended sediment, respectively. The proportions are consistent with expectations [36].

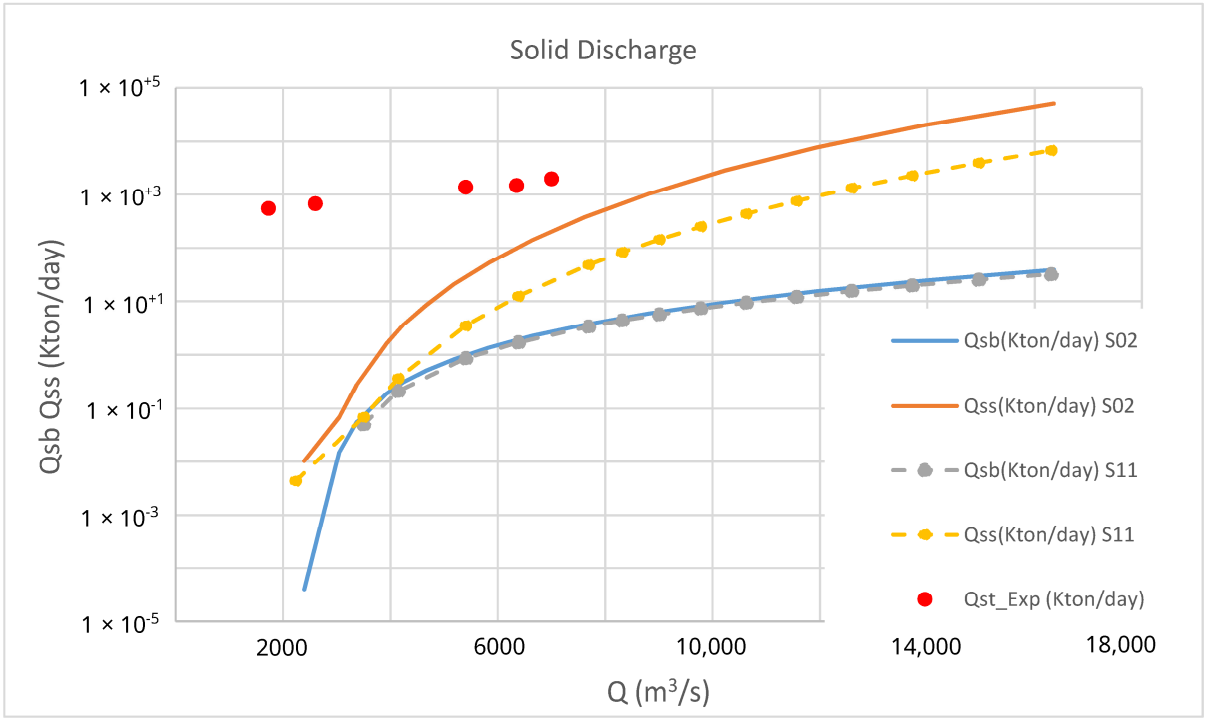

Figure 16. Solid bottom flow and suspension in sections S02 and S11.

3.4. Morphodynamic Characteristics of the Riverbed

The Magdalena River is a sinuous river with typical curvature radii at the end of its 5 km course, with a dominant flow of 7400 m^3/s and a solid flow of 1.7×10^5 m^3/day. The average grain size is 0.25 mm and the average Manning coefficient is 0.032. The usual bottom forms are large ripples for high flows and ripples for low flows. The dominant flow was calculated as the flow capable of continuously transporting solid material throughout the year as the total volume of solids transported by the river in an average hydrological year, consistent with sediment budget assessments conducted for the Magdalena basin [37].

Figure 17 shows a basic geometric description of the Magdalena riverbed over the last 40 km, showing how the radii of curvature are repeated in different parts of the

system, from upstream to downstream, except for the final part, which is a straight line of anthropogenic nature. The average radius of curvature is around 5 km, which can be used as a characteristic value for the riverbed, at least for the last 40 km.

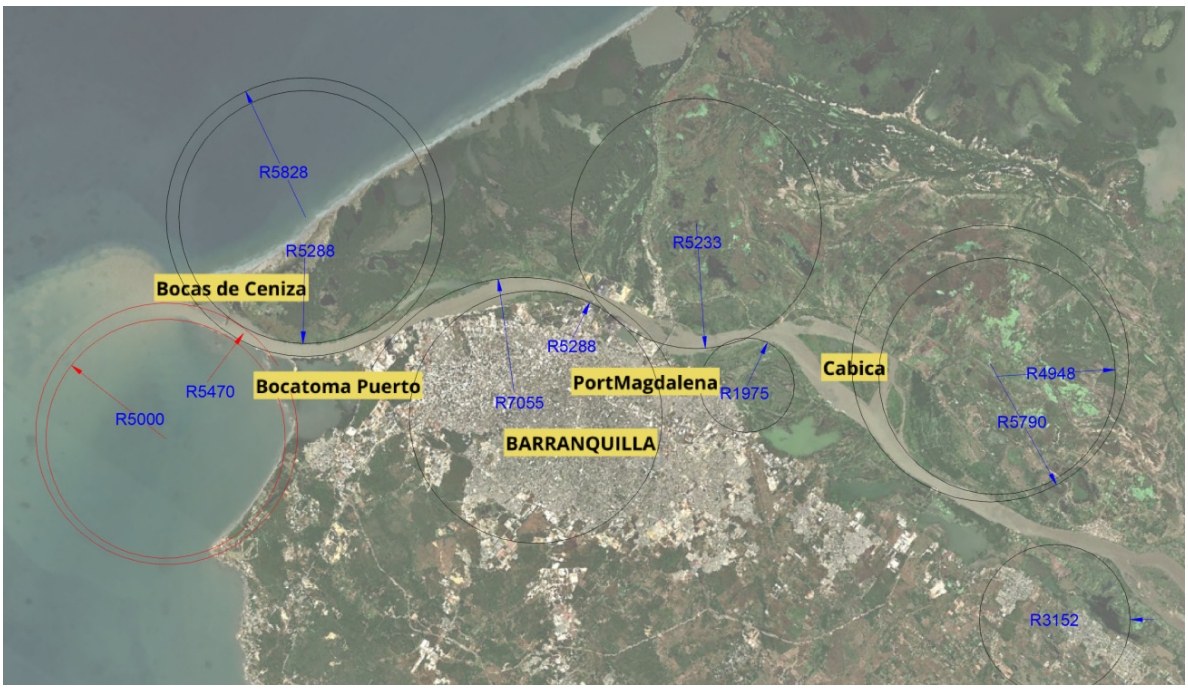

Figure 17. Radius of curvature of the last 40 km of the channel.

Along the riverbed, the Thalweg acquires a relative position that more or less conforms to Fargue's laws. However, in the presence of straight sections of anthropogenic origin, as in the case of the Magdalena, its position becomes misaligned and begins to wander through space and time. This occurs in the last few kilometers of the Magdalena River, as shown in Figure 17. The creation of a straight section causes random sedimentation in space and time in the form of bars and dunes, and the Thalweg begins to shift from one side to the other with the well-known consequences. It is not known where the Thalweg will be in the near future because of this instability. Above all, those that form at the mouth of the channel exacerbate by another phenomenon: the saline wedge that occurs at the mouth.

- On the saline wedge of the Magdalena

The salt wedge was measured at kilometer 21 upstream from Bocas de Ceniza, in accordance with typical mathematical calculations. The salt wedge is a flow of salt water that rises and falls according to the river's flow rate that comes from the Caribbean Sea. At low flow rates, the wedge moves upstream, and at high flow rates, it remains near the mouth of the river. Equilibrium occurs when the liquid flow is almost constant and the saline wedge remains stable in the same position. In these cases, the flow at the wedge has very low velocities and the bottom shear stresses are minimal, so if the sediment carried by the freshwater is able to cross the interface between the two media, saltwater and freshwater, by gravity, the sediment will be deposited on the bottom. For this reason, the salt wedge promotes the formation of sand bars and dunes in the mouth of the channel, which are part of the problem at Bocas de Ceniza. A study of the salt wedge with two layers, one of fresh water and one of salt water, has been carried out. The equations describing its movement were Saint Venant's equations with two superimposed immiscible currents. For high flows of 9000 m^3/s, the saline wedge is located between 60 and 400 m from the mouth, and for low flows of 3000 m^3/s, the wedge is located between 6000 and 8000 m.

- About the Thalweg

Control of a river channel lies in the control of the Thalweg itself, which is essential in channels used for navigation. Control of the Thalweg allows the route through the Thalweg, where ships sail the river, to be kept stable. In the Magdalena River, it is well known that before a ship enters, it must first be surveyed by a sounding vessel to indicate the most suitable position of the Thalweg for the incoming ship. Figure 18 shows that the Thalweg is stable at the exit of the previous bend, remains stable for a short distance after entering the straight section, and then becomes erratic. This occurs because the channel has been forced to flow in a straight line, which is unnatural. Rivers establish a certain curvature that forces the Thalweg to position itself on the outer side of the channel due to the secondary currents formed by the effect of the curvature, keeping its position stable. It would therefore be appropriate to use this knowledge to control the last part of the river.

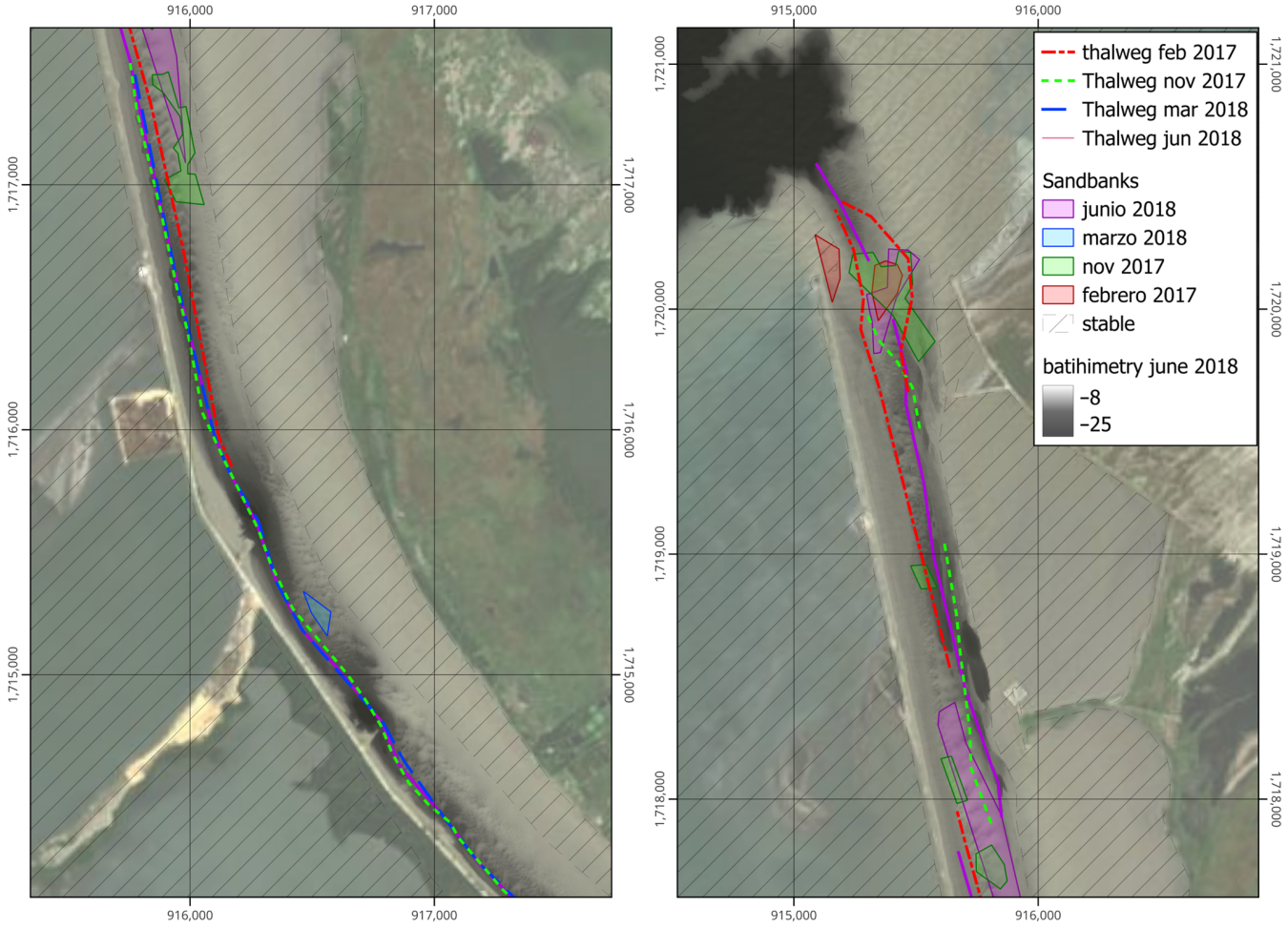

Figure 18. Thalweg disruption.

- About the dunes and the equilibrium slope.

As already mentioned, three detailed bathymetric surveys of the last 40 km of the river were carried out in December 2017, March 2018, and June 2018. The comparison between December 2017 and March 2018 is shown. For several months at the end of 2017, the flow remained fairly stable. A high flow was expected, but instead, during those months, it remained around the dominant flow. On the other hand, in March, the flow reached a minimum, but it was not stable. The flow changed gradually until it reached the minimum and then began to rise immediately, as can be seen in Figure 11. As a result, along the 40 km, the bed elevation profiles along the Thalweg are as shown in Figure 19.

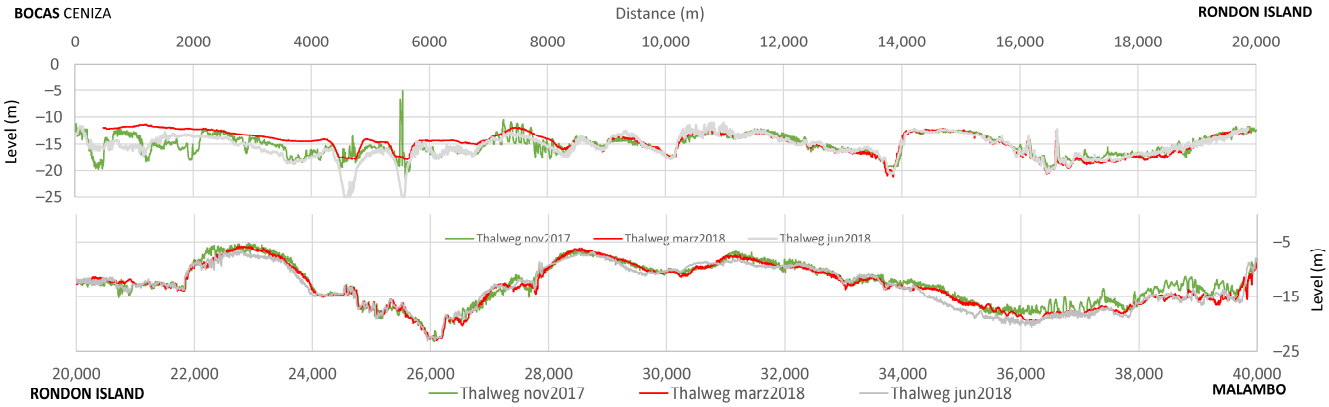

Figure 19. Bottom shapes along the last 40 km of the riverbed under two flow conditions, Green (November 2017—7500 m^3/s), blue (March 2018—3000 m^3/s) Gray (June 2018—7000 m^3/s).

The trend of the riverbed in the two flow situations is completely different. During the months when the river flow remained above 7400 m^3/s, a series of dunes and ripples formed along the entire riverbed. However, during low flows, the riverbed remained practically flat or formed much smaller dunes. The downstream contour condition has an interesting influence, as the flow meets the Caribbean Sea, which has a very low tide of 50 cm. At the mouth, the depth of the bed will be determined by the flow into the sea, as the width remains almost constant, delimited by the dikes and walls. This means that the bed will be deeper for higher flow rates and shallower for lower flow rates. It is interesting to note that the bottom in March 2018, with low flow, which is almost flat, is level with the crests of the dunes in December 2017, and in some areas even above them. The dunes that formed in December in this area are just over two meters high. Thus, the March 2018 riverbed is on average above the December 2017 riverbed near the mouth.

The situation remains relatively constant for a few kilometers; however, between kilometers 14 and 19, the riverbed measured in March 2018 is, on average, at the height of the dune crests observed in December. Between kilometers 19 and 21, in the Rondón Island area, the March riverbed is again above these crests. However, upstream of Rondón Island, the March 2018 bed is clearly below the December 2017 profile. This behavior is consistent with the fact that the average slope of the channel in December 2017 is greater than the mean slope recorded in March 2018, as would be expected.

Statistics were compiled for the dunes along the 40 km stretch at Table 4 shows the most relevant values from the statistics on the geometry of the dunes along the Thalweg. The number of dunes included in the statistics is sufficiently high to assess these characteristics. November is a good starting point due to its exceptional nature, with an almost constant flow of over 7000 m^3/s. In June, the flow was reaching similar values, but its trend came from very low values. On the other hand, in March 2018, the riverbed was at its lowest, with flows of 3400 m^3/s. As expected, the dunes are higher at high flows of 0.38 m and lower at low flows of 0.17 m. This is a notable difference. When the flow recovered in July, the dune heights were somewhat lower, at 0.28, which is consistent with the above. This is also reflected in the maximum heights. However, it should be noted that the Thalweg does not represent the spatial variation of the dunes in the riverbed, which are spectacular formations and require more detailed statistical analysis.

- On the minimum width of the channel for navigability

By considering the nature of the channel, as well as the equilibrium slopes and flow resistance as a function of flow rate, it is possible, based on these trends, to estimate the minimum width necessary to ensure adequate depth in the mouth area. Although this is an approximation, it allows us to understand the impossibility of continuing narrowing the

channel without compromising navigation conditions throughout the entire flow range, from 3000 to 10,000 m^3/s.

Table 4. Statistics on the geometric characteristics of the dunes.

Magnitudes in Meters	November 2017	March 2018	June 2018
Number of dunes	2426	2003	2599
Average height	0.38	0.17	0.28
Average length	5.78	6.14	5.42
Max height	4.57	3.54	3.33
Max Length	40.65	44.71	24.1

Table 5 presents the results of calculations performed under equilibrium conditions for different combinations of width and flow rate. It can be seen that, in order to maintain adequate depths at low flows adequate (for navigation desires), it would be necessary to reduce the width to around 250 m. However, with this flow section, the velocities associated with normal flows become excessively high, reaching values comparable to those recorded during flood events in the current situation, which would worsen navigation conditions. It is interesting to note that the average velocity for the dominant flow rate (7400 m^3/s) increases by 16% when the width is reduced, reaching 1.36 m/s. During wet months, when the flow exceeds 7400 m^3/s, this increase in velocity could make it difficult for vessels to enter to the Barranquilla Port in safe conditions.

Table 5. Channel limits to maintain adequate depths for navigation.

Q Barranquilla (m^3/s)	Q Calamar (m^3/s)	S_f	U (m/s)	n $s/m^{1/3}$	B (m)	h (m)	h (feet)
10,000	14,602	7.725×10^{-5}	1.55	0.035	425	15.1	49.7
10,000	14,602	7.725×10^{-5}	1.86	0.037	250	21.5	70.5
7400	9378	4.102×10^{-5}	1.17	0.033	425	14.8	48.6
7400	9378	4.102×10^{-5}	1.36	0.037	250	21.7	71.2
3000	2486	6.144×10^{-6}	0.81	0.013	425	8.8	28.7
3000	2486	6.144×10^{-6}	1.00	0.013	250	12.0	39.5

Nature-Based Solution

One of the main characteristics of rivers, resulting from hydrodynamic action, is the formation of longitudinal axis vortices parallel to the currents. These vortices generate lateral instability on the banks of the channels, causing sinuosity and, subsequently—in a feedback loop—the appearance of meandering channels.

The vortices alone consume an amount of power per unit of mass proportional to the cube of the average flow velocity and inversely proportional to the diameter of the flow, which is of the order of the depth of the channel. This energy initially comes from the differences between the bottom and bank forces, but is subsequently fed by the change in the direction of the river course.

The change in direction implies a variation in the flow of momentum, and this variation is exerted by the banks of the channel over the flow. This force is normal to the flow and is transmitted in to the interior of the water mass in the form of vorticity. The greater the curvature, the greater the force exerted by the bank and, therefore, the greater the vorticity generated within the flow.

Although a detailed analysis of this system gives rise to complex mathematical equations [37], it is possible to establish a simple overall relationship that allows us to understand how it works on average.

Figure 20 shows the overall balance of forces in a section of a meander or sinuosity, whose relationship is shown in Equation (5).

$$F = \sqrt{M_1^2 + M_2^2 - 2M_1 M_2 \cos\theta} \tag{5}$$

where F is the total force exerted by the channel bank on the flow to change its direction, θ is the angle by which the channel has turned due to the application of F, M is the momentum flow or specific force evaluated in the section as

$$M = \rho g \bar{h} A + \frac{\rho Q^2}{A} \tag{6}$$

where $\bar{h}$ is the centroid of the flow area, A, where the flow Q flows with a density ρ. For a flow in a meander of uniform section, the incoming and outgoing momentum flows are almost equal, so the value of force F is reduced to approximately $F = \sqrt{2}M\sqrt{1 - cos\theta}$, and the value of F is equal to M for a 60° turn of the flow. This would be the force that internally sustains the vortex within the flow, a quantity large enough to be considered.

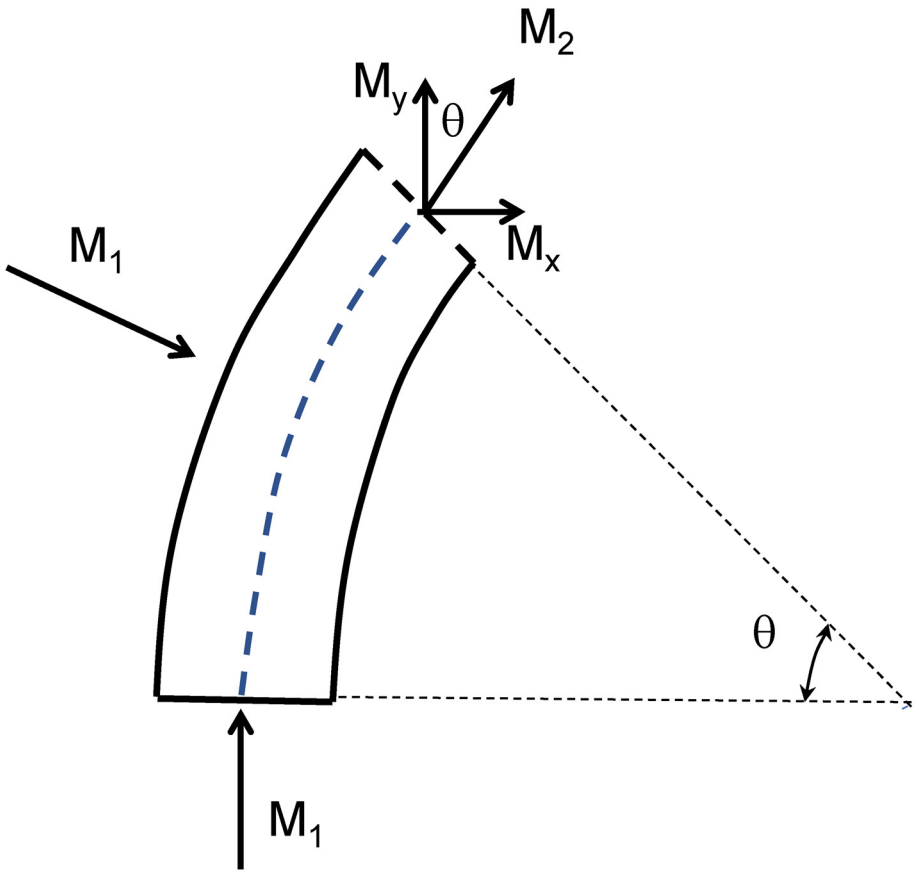

Figure 20. Assessment of the force that changes the flow of momentum in a channel.

Using this additional force, present within the flow, to combat various phenomena occurring at the mouth of the Magdalena River is what is called a nature-based solution. This force consists of a horizontal axis helical movement that rests on the outside of the curve, causing erosion of the outer bank. The material is transported transversely and

deposited on the inner bank of the meander. Thus, the outer bank is always deeper and is where the Thalweg is established.

The proposal consists of creating a final meander turning to the left at the mouth of the Magdalena River, eliminating the straight section that has been attempted to maintain in recent decades. This final meander will form a vortex that will address several problems. Specifically, it will help to deepen the riverbed without further narrowing the width of the Magdalena River. Secondly, it will help to keep the Thalweg stable over time, ensuring a constant navigation route with sufficient depth. Finally, it will combat the formation of the salt wedge, thus mitigating the generation of dunes in the mouth area.

Finally, this meander would be aligned with the underwater canyon, making it easier for the transported sediment to flow directly into it. This solution would reduce or even eliminate the frequency of dredging maintenance in the area. Although it does not completely prevent future collapses of the material deposited on the edge of the canyon—which will continue to occur—it will allow the depth level to be kept under greater control.

3.5. Design and Assessment of the New Meander at Bocas de Ceniza

Figure 21 presents the design of the new meander, located in the final reach of the navigation channel approaching the mouth of the Magdalena River. The existing meander was extended by 1 km, maintaining the same radius of curvature. Subsequently, a 1 km transition was laid out, leading to the final left-hand bend. This last curved reach will behave in a manner analogous to the previous one, but symmetrically, ultimately directing the flow toward the submarine canyon.

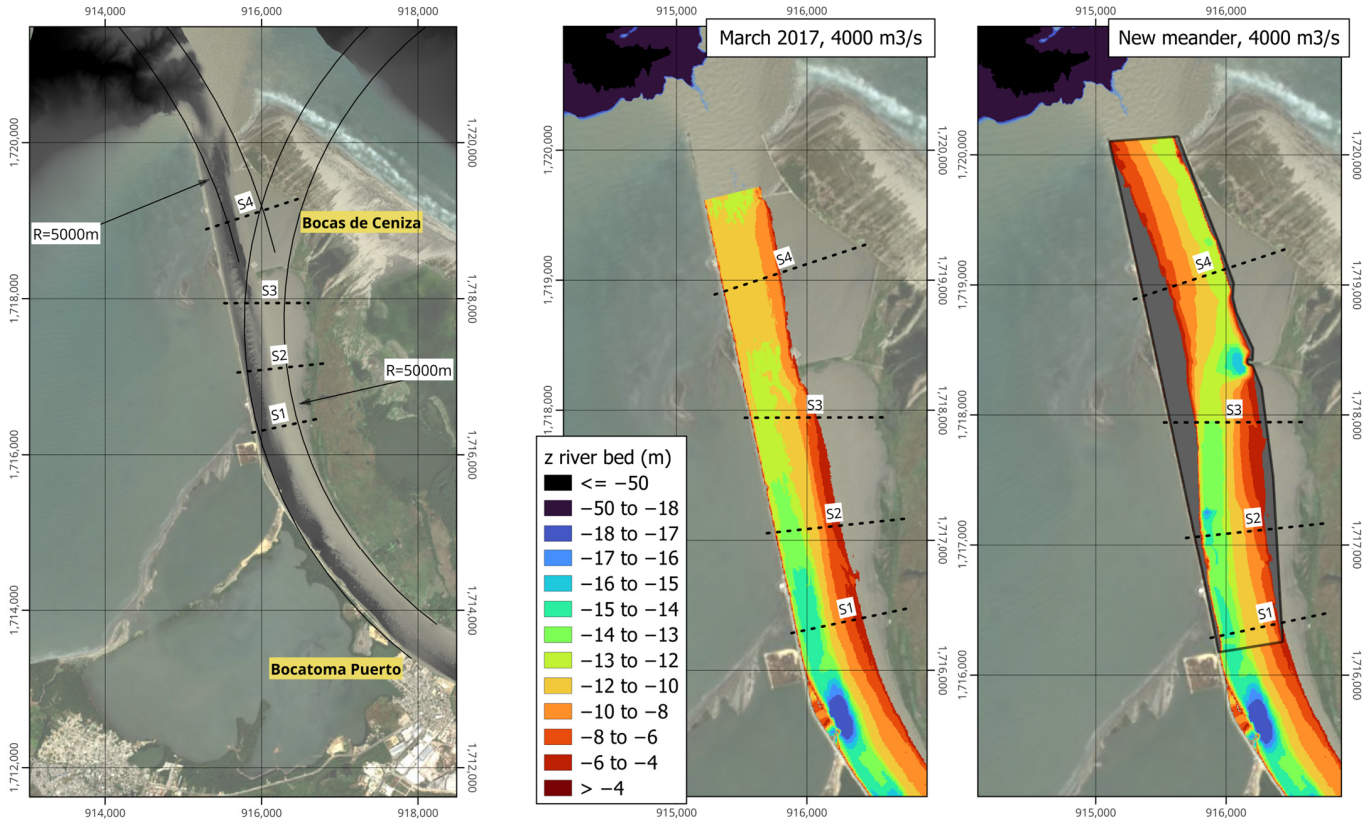

Figure 21. Proposed alignment of the new meander and a comparison before and after the implementation of it.

To implement this new alignment, the removal of spur dike 6 is required, while the guide dike must be shortened, taking advantage of the induced local erosion to increase

the depth of the navigable channel at the change in curvature of the alignment. This approach is based on using natural morphodynamic conditions as the foundation of the proposed solution.

Figure 21 also includes a comparison of the channel configuration before and after the implementation of the new meander under low-flow conditions, which represent the most critical scenario for river navigability.

As previously indicated, fully resolved numerical modeling of the new meander is highly complex and remains computationally challenging. Two-dimensional models are unable to adequately represent secondary currents and therefore cannot reliably simulate sediment transport or erosion processes in bends. On the other hand, the hydraulic and sediment transport problem is of excessive scale and complexity to be addressed using a three-dimensional model. Consequently, an alternative approach was adopted for the evaluation of the new meander, based on solutions already provided by natural river behavior.

Immediately upstream of Bocas de Ceniza and the newly designed meander lies the Bocatoma del Puerto reach. The channel in this area exhibits geometric characteristics very similar to those of the new alignment, as the latter was designed by maintaining channel widths and radii of curvature equivalent to those observed at Bocatoma del Puerto (see Figure 22). Therefore, it was considered appropriate to replicate the bed morphology of the Bocatoma del Puerto bend in the Bocas de Ceniza area, thereby obtaining a representation of the bed of the new meander based on measured field data, without the need for numerical modeling.

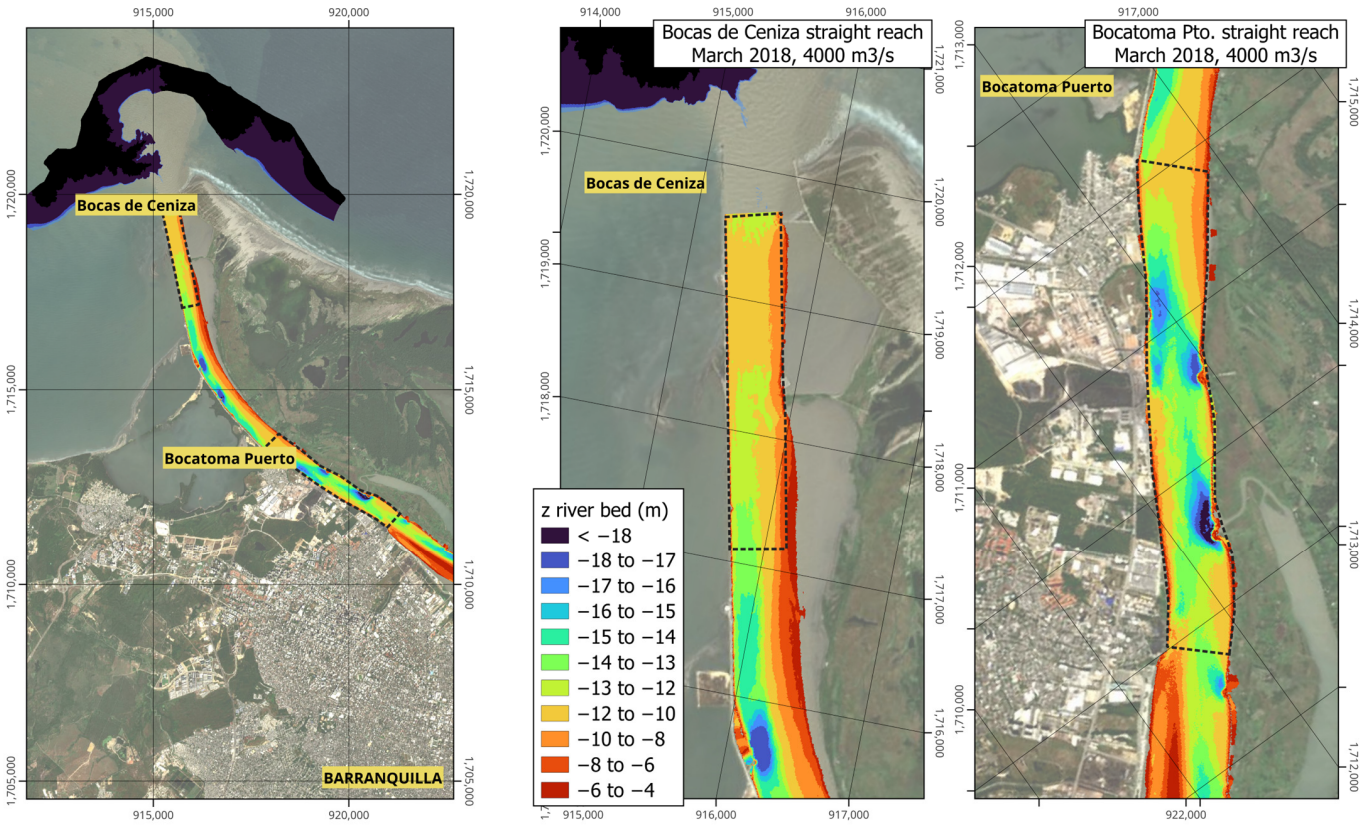

Figure 22. Comparison between the straight reaches of Bocas de Ceniza and Bocatoma Puerto.

Nevertheless, there is a significant difference between the two reaches: Bocas de Ceniza is strongly influenced by the presence of the salt wedge, whereas Bocatoma del Puerto is affected by this phenomenon only under exceptionally low discharges. To estimate the

magnitude of this effect, a comparison was carried out between the straight reach at Bocas de Ceniza and the straight reach located between Bocatoma del Puerto and El Palmar. Both reaches have been canalized with very similar characteristics. The Bocatoma del Puerto reach extends over several kilometers and has an average width of approximately 490 m, formed by a series of dikes, compared to an average width of about 480 m at Bocas de Ceniza. The most relevant difference between the two reaches is therefore the presence of the salt wedge at Bocas de Ceniza.

From this comparison of the straight reaches, a difference in mean bed elevation (Δz) associated with the salt-wedge effect was identified (see Table 6). This difference is used to correct the replicated bed elevation as it approaches the sea (see Equation (7)).

$$z\ replica,\ new\ meander\ \approx z\ meander, Boc.Pto. + (z\ straight,\ Boc.\ Pto. - z\ straight,\ Bocas\ Ceniza) \quad (7)$$

Table 6. Mean bed elevation difference between the Bocatoma Puerto and Bocas de Ceniza straight reaches.

	z Mean Bocatoma Puerto Straight (m)	z Mean Bocas Ceniza Straight (m)	Δz (m)
nov-17	−13.69	−13.16	0.53
mar-18	−13.48	−11.43	2.05

Figures 21 and 23 show a comparison between the existing channel bed and the design of the new meander obtained through the replication procedure described above. This comparison confirms that the proposed configuration, together with its radii of curvature, maintains the Thalweg in a stable position and allows depths on the order of 1 m greater than those of the current configuration to be achieved (see Figure 23).

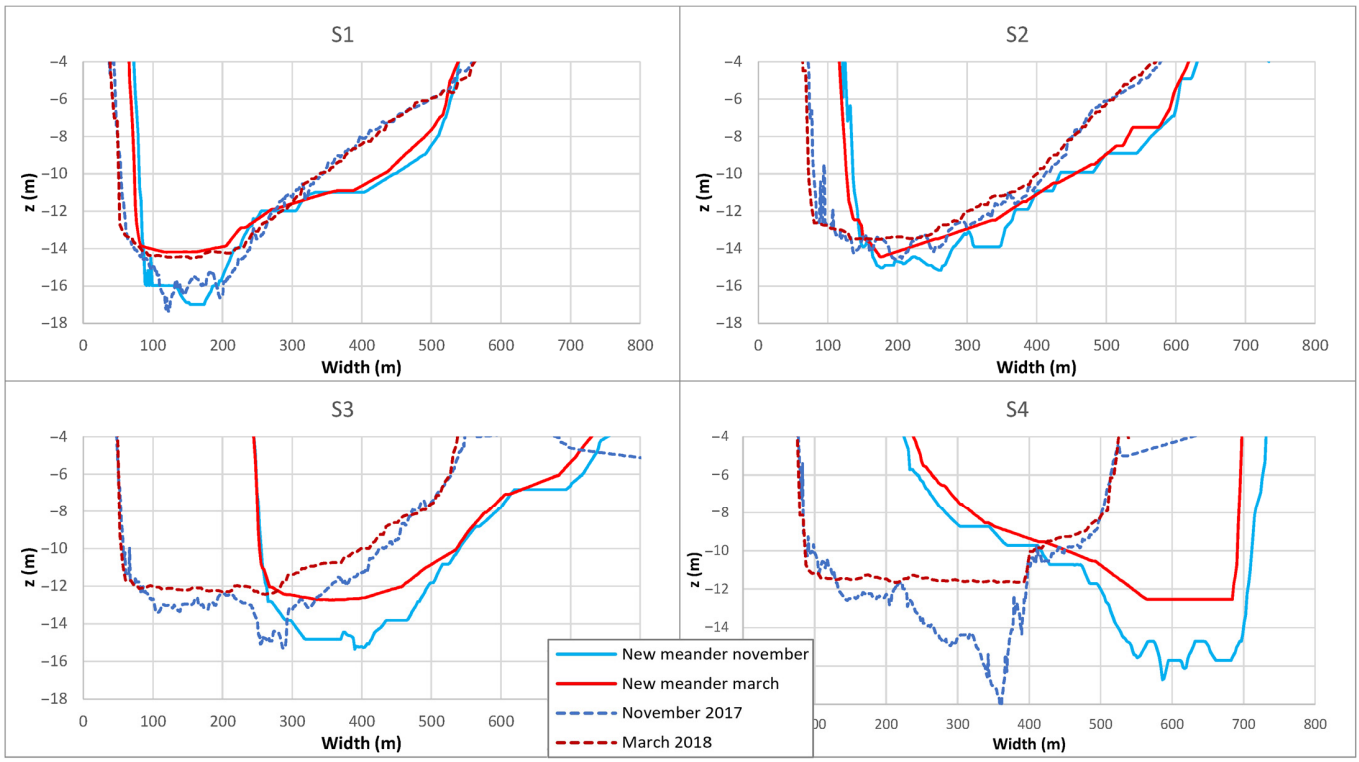

Figure 23. Comparison between the existing channel bed and the design of the new meander obtained from the replication procedure.

4. Discussion

4.1. Controls on Thalweg Instability in Trained River Mouths

River mouths are highly dynamic environments in which the fluvial system continuously adjusts toward a transient equilibrium state. This adjustment reflects the balance between liquid discharge, sediment supply, bed slope and grain size, which jointly control flow depth, sediment transport capacity, and channel morphology. Although a true equilibrium could only be achieved under constant discharge—an unrealizable condition in natural rivers—the tendency toward adjustment remains operative over a wide range of hydrological conditions.

Under approximately constant downstream water-level conditions, such as those imposed by sea level at river mouths, variations in river discharge induce systematic alternations between erosion-dominated and deposition-dominated states. An increase in discharge enhances sediment transport capacity, promoting bed degradation at the outlet and triggering upstream-migrating erosional responses associated with an increase in energy slope. Conversely, decreasing discharge favors sediment deposition near the river mouth, reducing the local energy gradient and, on average, lowering channel slope upstream. This cyclic erosion–deposition behavior plays a key role in controlling channel stability, particularly in engineered and laterally constrained reaches.

In artificially straightened or laterally confined channels, the flow tends to develop weak secondary circulation patterns, often manifested as longitudinal vortices induced by shear differences between the bed and the sidewalls. These circulation cells may intermittently generate lateral scour zones near the margins and zones of sediment accumulation near the channel center. However, such secondary flow structures are inherently unstable and highly sensitive to changes in discharge and bed configuration. As a result, relatively small perturbations may lead to the weakening or disappearance of one or both circulation cells, producing abrupt lateral shifts of the thalweg.

This mechanism provides a plausible explanation for the thalweg instability observed in the rectified reach of the Magdalena River. Field observations indicate lateral thalweg migration associated with discharge variations between approximately 7400 m^3/s and 3000 m^3/s. Although temporary stabilization may occur under specific flow conditions, the resulting behavior remains inherently unsteady. Consequently, straightened configurations in this reach are unsuitable for providing reliable and persistent navigation conditions. Similar morphodynamic responses to channel straightening have been documented in gravel-bed rivers, where imposed rectification leads to longitudinal slope adjustment, bar reorganization, and increased bed instability [38,39].

4.2. Interaction Between Salt-Wedge Dynamics and Morphodynamics

In river mouths influenced by marine conditions, the interaction between fluvial discharge and saline intrusion introduces an additional mechanism controlling bed morphology and channel stability. The salt wedge is driven upstream by the density contrast between seawater and freshwater, which results in a higher near-bed pressure relative to the overlying freshwater and drives an upstream-directed force along the channel bottom. This upstream motion is opposed by the downstream momentum flux of the river flow. High discharges are therefore capable of displacing the salt wedge seaward, whereas lower or more stable discharges favor the development of a quasi-stationary saline intrusion extending upstream from the river mouth.

Freshwater flows above the saline layer, generating shear at the interface between the two water bodies. This interfacial shear balances the pressure difference associated with density stratification and controls the longitudinal position of the salt wedge. The saline body beneath the interface, which remains in direct contact with the channel bed, is

characterized by very low flow velocities and therefore exerts only negligible bed shear stress at the channel bottom. Under these low-velocity conditions, bed shear stresses do not exceed the critical Shields threshold for the initiation of sediment motion, and deposition of solid material is therefore promoted.

As a result, sediment tends to accumulate near the bed, favoring the formation of bars along the channel margins and progressively restricting navigability in the affected reach. These depositional features are commonly removed through frequent dredging operations to maintain vessel access. Under sustained high discharges, dunes and bars tend to be confined to the vicinity of the river mouth. In contrast, during prolonged low-discharge periods, the salt wedge elongates upstream, extending the zone of reduced bed shear stress and promoting bar formation over a much larger river reach influenced by saline intrusion.

The structure of the salt wedge is dynamically robust and difficult to disrupt through natural mixing processes. One of the few mechanisms capable of enhancing mixing between freshwater and saline water is the development of secondary circulation. These currents generate longitudinal circulation cells, typically supported along the outer bank of channel bends, which promote vertical and lateral exchange across the density interface. Straightened channels inhibit the development of such secondary circulation, whereas channel curvature or planform sinuosity enhances mixing and reduces the persistence of salt-wedge-induced depositional zones.

4.3. Limits of Channel Narrowing as a Navigation Strategy

In general, river channels tend to deepen and widen as discharge increases, reaching an average equilibrium associated with a characteristic flow commonly referred to as the dominant or morphological discharge. However, in most alluvial rivers, channel widening occurs at a faster rate than channel deepening as discharge increases. This asymmetric geometric adjustment reflects fundamental morphodynamic constraints and limits the effectiveness of channel narrowing as a strategy to increase navigable depth.

Any intervention acting on channel boundaries, such as an artificial reduction in channel width, therefore has immediate consequences for flow depth and velocity. Channel narrowing tends to induce local bed deepening; however, because the width–depth relationship is highly non-linear and operates at different rates, achieving a given increase in depth requires a disproportionately large reduction in channel width. This effect can be quantified using the dimensionless relationships that describe channel geometry at the morphological discharge, given by $\hat{B} = 0.274\ \hat{Q}^{5.65}$ and $\hat{H} = 3.01\ \hat{Q}^{0.321}$.

By substituting the dimensionless discharge from one expression into the other and differentiating the dimensionless depth with respect to the dimensionless width, the following relationship is obtained: $d\hat{H} = 0.17\left(\frac{0.274}{\hat{B}}\right)^{0.943} d\hat{B}$ For a representative channel width of approximately 400 m, this relationship yields $d\hat{B} = 5668\ d\hat{H}$.

Although this estimate is approximate, it clearly illustrates the strong disparity between reductions in channel width and the resulting increases in channel depth. In practical terms, modest gains in navigable depth would require unrealistically large reductions in channel width, rendering channel narrowing an inefficient and potentially counterproductive strategy for navigation improvement.

In addition, progressive channel narrowing leads to an increase in mean flow velocity. While higher velocities may enhance sediment transport capacity, they can also impose operational constraints on upstream vessel navigation and increase hydrodynamic loading on river training structures. More importantly, channel narrowing does not address the fundamental processes governing sediment deposition and thalweg instability in straightened river mouths. Although simplified two-dimensional hydrodynamic modeling was employed as an exploratory tool, the processes governing thalweg stabilization and sediment

redistribution in curved channels under saline intrusion are inherently three-dimensional. In particular, secondary circulation and transverse sediment transport—which play a central role in the proposed approach—cannot be adequately represented within a depth-averaged framework. Consequently, the present analysis does not aim at a quantitative prediction of long-term morphodynamic evolution, but rather at identifying process-based design principles consistent with observed stable river configurations.

By contrast, channel curvature promotes the development of coherent secondary flow structures and transverse sediment transport, leading to a spatial concentration of bed shear stress within the channel cross-section. This localized increase in bed shear stress favors selective bed deepening along the thalweg without requiring additional channel confinement. These mechanisms indicate that planform geometry, rather than further confinement, plays a central role in achieving stable and navigable channel configurations.

4.4. Nature-Based Solution as a Process-Based Design

Nature-based solutions in fluvial systems should not be interpreted as purely ecological or landscape-oriented interventions, but rather as process-based designs grounded in the intrinsic dynamics that govern river morphology. River geometry emerges from long-term adjustments between flow, sediment transport, and boundary conditions, leading to configurations that are dynamically stable under prevailing hydrological regimes.

From this perspective, the objective is not to introduce natural elements because they are perceived as "natural", but to identify, quantify, and reproduce geomorphic configurations that have already demonstrated stability under comparable forcing conditions. Unaltered or weakly disturbed river reaches therefore constitute full-scale, long-term experiments, in which channel geometry, curvature, width, depth, slope, and planform have been selected by the river itself through sustained morphodynamic adjustment.

When a river reach must be redesigned, the most robust strategy is to identify a nearby reference reach with similar discharge and sediment characteristics, measure its geometric and morphodynamic properties, and transfer these features to the altered section. This approach relies on the assumption that the reference reach represents a near-equilibrium solution for the given boundary conditions and thus minimizes the risk of unintended morphodynamic responses following intervention.

In the case of the Magdalena River, the downstream reach has been artificially constrained by engineering works such as groynes and dikes, with the objective of maintaining a straight channel for navigation. Field observations, however, indicate that this imposed configuration is unstable: the thalweg exhibits pronounced lateral mobility and the channel persistently tends to re-establish curvature. This behavior suggests that the current geometry is incompatible with the dominant fluvial and estuarine processes acting at the river mouth.

By contrast, the upstream meandering reach provides a clear reference for the geometry that the river naturally tends to develop under comparable hydrological and sedimentary conditions. Reproducing this meander in the downstream section, in a specular or adapted form, constitutes a process-based nature-based solution aligned with the inherent morphodynamic tendencies of the system. Rather than forcing the river into an artificial equilibrium, such an intervention facilitates the configuration that the river itself seeks to establish, thereby enhancing long-term stability and navigability.

The main challenge associated with this approach lies in the construction phase, which requires specific techniques to reproduce the target geometry while controlling short-term instabilities. Nevertheless, once implemented, the solution relies primarily on natural adjustment processes to maintain its functionality over time, reducing the need for continuous corrective interventions such as dredging and structural reinforcement.

5. Conclusions

The history of the morphological changes that the Magdalena River has undergone in the last 100 years shows that the only way to achieve greater depth in the Magdalena River has been at the cost of narrowing the channel, a strategy that has been pursued to the present day. These findings demonstrate that the channel cannot be narrowed indefinitely, as doing so increases mean flow velocities to values that are practically unusable for vessel traffic, which is ultimately the purpose of the works. Navigational risk for ships entering Bocas de Ceniza is further exacerbated under high-velocity conditions. In addition, spur dike 6 induces unstable flow at the outlet, generating vortex structures with horizontal and vertical axes that propagate throughout the flow field. This study confirms that the practical narrowing limit has been reached; further increases in velocity cannot be tolerated without placing vessels at risk.

The river has undergone substantial morphological alteration, a delta formed by a series of islands that likely supported an important biotic component, which has now disappeared from the system. The delta vanished when the eastern and western dikes began to be constructed, and, in order to improve conveyance, several large channels diverting flow toward the Santa Marta marsh were cut off, thereby increasing discharge concentration and channel depth.

This study documents the hydrodynamic characteristics that can be used for future analyses, as it provides relationships among discharge, water level, driving slope, and roughness. With these data, engineers and researchers have a robust basis for more accurate calculations. The Magdalena River, known as Kariguaña by Indigenous communities, currently exhibits a formative discharge of approximately 7400 m^3/s, with a total sediment transport on the order of 2000 kt/day. The flow resistance coefficient is around 0.021 under low-flow conditions and approximately 0.034 during high flows. The average curvature radii are on the order of 5000 m, the maximum driving slope measured in the natural reach is about 1.2×10^{-5}, and in the port area it reaches values of up to 1×10^{-4}. Under high-flow conditions, dunes exceeding 2 m in height have been measured, forming organized dune fields along the studied reach; under low-flow conditions, dunes exhibit average wavelengths less than half of those observed during high flows.

An important result is that the correlation between measured velocity profiles and driving slope can only be achieved if the value of the von Kármán coefficient decreases. For low flows, it varies within a lower range, whereas for high flows it reaches higher values. This behavior can be partly explained by the influence of high near-bed sediment concentrations.

From a morphological perspective, the instability of the thalweg in straight channels is demonstrated, highlighting the difficulty of maintaining a navigable channel that remains fixed over time. Channel bends with radii of approximately 5000 m provide a useful reference for designing a more natural planform at the mouth of the Magdalena River. Such a configuration would enhance thalweg stability, promote additional channel deepening relative to current conditions, and improve mixing of the saline wedge, thereby mitigating sedimentation in the near-mouth region. An additional objective is to guide the main flow toward the offshore submarine canyon, creating more favorable conditions for vessel entry by aligning channel depths with canyon bathymetry.

Riverbed morphology is governed by the interaction between liquid discharge, sediment transport, and grain-size characteristics, while anthropogenic interventions attempt to modify this equilibrium. In some cases, such modifications can be accommodated by natural processes; however, rivers have finite physical limits. The Magdalena—or Kariguaña—River cannot be further narrowed without compromising bed stability and impairing navigability. The most viable alternative is therefore to modify the planform by introducing greater sinuosity, thereby establishing a more stable thalweg and achieving

increased depths without exceeding the system's intrinsic limits. Few navigation ports worldwide are located at the mouths of rivers as morphodynamically energetic as the Magdalena, making this case exemplifies the broader challenge of maintaining adequate navigation depths in highly dynamic river–estuary systems.

Author Contributions: Conceptualization, A.B.P.; Methodology, A.B.P. and R.S.P.; Formal analysis, A.B.P. and R.S.P.; Investigation, A.B.P. and R.S.P.; Data curation, R.S.P.; Visualization, R.S.P.; Writing—original draft preparation, A.B.P.; Writing—review and editing, A.B.P. and R.S.P.; Supervision, A.B.P.; Project administration, A.B.P. All authors have read and agreed to the published version of the manuscript.

Funding: This study was developed under contract CT 828—2017. Additional technical collaboration and institutional support were provided by the Ministry of Transport (INVÍAS), and WEG Engineering.

Institutional Review Board Statement: Not applicable.

Informed Consent Statement: Not applicable.

Data Availability Statement: The raw data supporting the conclusions of this article will be made available by the authors on request.

Acknowledgments: The Ministry of Transport INVIAS, WEG Engineering and the National University of Colombia, Medellin campus were fundamental to the development of this innovative project.

Conflicts of Interest: The authors declare no conflicts of interest.

References

1. Church, M.; Ferguson, R.I. Morphodynamics: Rivers beyond steady state. *Water Resour. Res.* **2015**, *51*, 1883–1897. [CrossRef]
2. Wilkerson, G.V.; Parker, G. Physical basis for quasi-universal relationships describing bankfull hydraulic geometry of sand-bed rivers. *J. Hydraul. Eng.* **2011**, *137*, 739–753. [CrossRef]
3. Parker, G. On the cause and characteristic scales of meandering and braiding in rivers. *J. Fluid Mech.* **1976**, *76*, 457–480. [CrossRef]
4. Mosselman, E. Studies on river training. *Water* **2020**, *12*, 3100. [CrossRef]
5. Le, T.B.; Crosato, A.; Montes Arboleda, A. Revisiting Waal river training by historical reconstruction. *J. Hydraul. Eng.* **2020**, *146*, 05020002. [CrossRef]
6. Ikeda, S. Lateral bed load transport on side slopes. *J. Hydraul. Div.* **1982**, *108*, 1369–1373. [CrossRef]
7. Dietrich, W.E.; Smith, J.D. Influence of the point bar on flow through curved channels. *Water Resour. Res.* **1983**, *19*, 1173–1192. [CrossRef]
8. Blanckaert, K.; de Vriend, H.J. Secondary flow in sharp open-channel bends. *J. Fluid Mech.* **2004**, *498*, 353–380. [CrossRef]
9. Kleinhans, M.G.; van den Berg, J.H. River channel and bar patterns explained and predicted by an empirical and a physics-based method. *Earth Surf. Process. Landf.* **2011**, *36*, 721–738. [CrossRef]
10. Mahgoub, M.; Hinkelmann, R.; La Rocca, M. Understanding the behaviour of gravity currents in tideless estuaries and considering the impact of sea level rise within the Nile Estuary. *J. Coast. Res.* **2015**, *31*, 714–722. [CrossRef]
11. La Rocca, M.; Adduce, C.; Sciortino, G.; Pinzón, A.B. Experimental and numerical simulation of three-dimensional gravity currents on smooth and rough bottom. *Phys. Fluids* **2008**, *20*, 106603. [CrossRef]
12. Nanson, G.C.; Knight, D.W. Anabranching rivers: Their cause, character and classification. *Earth Surf. Process. Landf.* **1996**, *21*, 217–239. [CrossRef]
13. Restrepo, J.C.; Orejarena-Rondón, A.; Consuegra, C.; Pérez, J.; Llinas, H.; Otero, L.; Álvarez, O. Siltation on a highly regulated estuarine system: The Magdalena River mouth case (Northwestern South America). *Estuar. Coast. Shelf Sci.* **2020**, *245*, 107020. [CrossRef]
14. PIANC. *Working with Nature: Position Paper (Original 2008; Revised January 2011)*; The World Association for Waterborne Transport Infrastructure (PIANC): Brussels, Belgium, 2011.
15. King, J.K.; Suedel, B.C.; Bridges, T.S. Achieving sustainable outcomes using engineering with nature principles and practices. *Integr. Environ. Assess. Manag.* **2020**, *16*, 546–548. [CrossRef] [PubMed]
16. Cohen-Shacham, E.; Walters, G.; Janzen, C.; Maginnis, S. *Nature-Based Solutions to Address Global Societal Challenges*; IUCN: Gland, Switzerland, 2016; Volume 97, p. 2036.

17. Konsoer, K.M.; Rhoads, B.L.; Best, J.L.; Langendoen, E.J.; Abad, J.D.; Parsons, D.R.; Garcia, M.H. Three-dimensional flow structure and bed morphology in large elongate meander loops with different outer bank roughness characteristics. *Water Resour. Res.* **2016**, *52*, 9621–9641. [CrossRef]
18. Schuurman, F.; Kleinhans, M.G. Bar dynamics and bifurcation evolution in a modelled braided sand-bed river. *Earth Surf. Process. Landf.* **2015**, *40*, 1318–1333. [CrossRef]
19. Galloway, W.E. Process Framework for Describing the Morphologic and Stratigraphic Evolution of Deltaic Depositional Systems. In *The AAPG/Datapages Combined Publications Database*; Houston Geological Society: Houston, TX, USA, 1975.
20. Rico Pulido, E. Las Obras de Bocas de Ceniza. Communication of Puertos de Colombia, 1967.
21. Restrepo, J.D.; Syvitski, J.P.M. Assessing the effect of natural controls and land use change on sediment yield in a major South American drainage basin. *Basin Res.* **2006**, *18*, 89–101.
22. Sir Alexander Gibb & Partners. *Report on Studies of River Training. Works at Bocas de Ceniza from 1929 to 1966*; Blanco, J., Ed.; Obras Completas I; Original Report: 30 November 1959; Universidad del Norte: Barranquilla, Colombia, 1966.
23. Galera Ruiz, D. Dynamics of Submerged Granular Flow. Bachelor's Degree Thesis in Civil Engineering, Barcelona, Spain, 2011.
24. Restrepo, J.D.; Escobar, H.A.; López, S.A.; Tosic, M. Morphodynamics and sediment transport in a tropical delta system: The Magdalena River, Colombia. *J. Coast. Res.* **2016**, *32*, 635–649.
25. Viparelli, E.; Blom, A.; Ferrer-Boix, C.; Kuprenas, R. Comparison between experimental and numerical stratigraphy emplaced by a prograding delta. *Earth Surf. Dyn.* **2014**, *2*, 323–338. [CrossRef]
26. Wolf, S.; Esser, V.; Schüttrumpf, H.; Lehmkuhl, F. Influence of 200 years of water resource management on a typical central European river. Does industrialization straighten a river? *Environ. Sci. Eur.* **2021**, *33*, 15. [CrossRef]
27. Gómez-Dueñas, S.; Bateman, A.; Santos Granados, G.R. Untangling the implications of climate-forcing and human-induced drivers in streamflow variability: The Magdalena River, Colombia. *Hydrol. Sci. J.* **2024**, *69*, 1046–1059. [CrossRef]
28. Cortés, A.F.; Bateman, A.; Medina, V. Drought Characterization for the Ciénaga Grande de Santa Marta (Colombia). In *Proceedings of the 8th IAHR Europe Congress, Lisbon, Portugal, 4–7 June 2024*; Book of Abstracts 30957; IAHR: Madrid, Spain, 2024.
29. Gaudio, R.; Miglio, A.; Dey, S. Non-universality of von Kármán's κ in fluvial streams. *J. Hydraul. Res.* **2010**, *48*, 658–663. [CrossRef]
30. Gómez-Dueñas, S.; Bateman, A.; Santos Granados, G.R. Determining a wetland inflow threshold: A proxy gauge station approach in Ciénaga Grande de Santa Marta, Colombia. *Hydrol. Sci. J.* **2025**, *70*, 1686–1699. [CrossRef]
31. Restrepo, J.D.; Kjerfve, B. Magdalena River: Interannual variability (1975–1995) and revised sediment load estimate. *J. Hydrol.* **2000**, *235*, 137–149. [CrossRef]
32. Parker, G. *1D Sediment Transport Morphodynamics with Applications to Rivers and Turbidity Currents*; This is an e-book with PowerPoint presentations, Excel worksheets with embedded working programs in Visual Basic for Applications, Word files with extended explanation and video clips; IAHR Media Library: Online, 2004.
33. Wright, S.; Parker, G. Grain-size specific suspended sediment transport and flow resistance in large sand-bed rivers. In *Sedimentation and Sediment Transport*; Springer: Dordrecht, The Netherlands, 2003; pp. 221–227.
34. Garcia, M.; Parker, G. Experiments on the entrainment of sediment into suspension by a dense bottom current. *J. Geophys. Res. Ocean.* **1993**, *98*, 4793–4807. [CrossRef]
35. Coleman, N.L. Velocity profiles with suspended sediment. *J. Hydraul. Res.* **1981**, *19*, 211–229. [CrossRef]
36. Higgins, A.; Restrepo, J.C.; Ortiz, J.C.; Pierini, J.; Otero, L. Suspended sediment transport in the Magdalena River (Colombia, South America): Hydrologic regime, rating parameters and effective discharge variability. *Int. J. Sediment Res.* **2016**, *31*, 25–35. [CrossRef]
37. Fisher, R.A. Sediment Budget Framework Applied to the Magdalena River Basin. Master's Thesis, University of Montana, Missoula, MT, USA, 2020.
38. Talbot, T.; Lapointe, M. Modes of response of a gravel bed river to meander straightening. *Water Resour. Res.* **2002**, *38*, 9-1–9-7. [CrossRef]
39. Talbot, T.; Lapointe, M. Numerical modeling of gravel bed river response to meander straightening: The coupling between the evolution of bed pavement and long profile. *Water Resour. Res.* **2002**, *38*, 10-1–10-10. [CrossRef]